Rivista Italiana di Paleontologia e Stratigrafia	volume 121	no. 3	pp. 345-368	November 2015

TRANSPORTED RHODOLITHS WITNESS THE LOST CARBONATE FACTORY: A CASE HISTORY FROM THE MIOCENE PIETRA DA CANTONI LIMESTONE (NW ITALY)

GIOVANNI COLETTI* [1], DANIELA BASSO [1], ALFREDO FRIXA [2] & CESARE CORSELLI [1]

Received: January 08, 2015; accepted: September 08, 2015

Key words: Rhodoliths, coralline algae, rhodalgal carbonate factory, transport, barnacle, glaucony, phosphates.

Abstract. Inner-platform bioclasts may have a remarkable preservation potential when transported toward deeper and quieter basin environments. Rhodoliths can bind skeletal grains during their growth, thereby storing information on their native environment even after transport. The Burdigalian Pietra da Cantoni Group (Piedmont, NW Italy) has been analyzed as an example of lost carbonate factory, to stress the rhodolith potential in studies of displaced sediments and within this framework an overview of the main mechanisms of rhodolith transport is provided. The examined successions testify the progressive sediment starvation of the middle and outer ramp caused by the interruption of shallow-water sediment supply due to sea-level rise. Four facies have been identified: Facies 1 is a coarse limestone characterized by inner-middle ramp rhodalgal skeletal assemblages deposited on the lower middle-ramp; Facies 2 is an impure limestone linked to the inception of sediment starvation; Facies 3 is a glauconitic-phosphatic marly-limestone that marks the end of sediment supply from shallow-water to the lower middle-ramp; Facies 4 is a marly limestone that represents the beginning of hemipelagic sedimentation. The sediment has been displaced toward a deeper setting from its source area, reconstructed as a high-energy and turbid shallow-water environment. The skeletal debris trapped inside the rhodoliths are related to an inner-middle ramp setting and have faithfully witnessed the environment of rhodolith formation.

Introduction

This work is aimed at improving our knowledge of fossil rhodalgal factories by emphasizing rhodoliths as a tool in the study of transported sediments. The Pietra da Cantoni Group (PDC; Lower Miocene) of the Tertiary Piedmont Basin (TPB) (Schüttenhelm 1976; Vannucci et al. 1996; Bicchi et al. 2002; Bicchi et al. 2006) has been chosen as an example of a rhodalgal carbonate platform, where the main area of carbonate production is not flawless preserved in place. In this framework we analyze and integrate literature data and new observations on the paleontology and sedimentology of the PDC and we review the mechanisms and processes involved in rhodolith transport.

From the Oligocene onward, coralline algae have spread massively throughout the platform photic zone. Because they are well adapted to a broad range of climatic conditions and can thrive even in dim light, they are one of the most common and important carbonate producers in platform environment. Coralline algae dominate in the rhodalgal carbonate factories (Carannante et al. 1988) where they are the main carbonate producers. During the Miocene these carbonate factories were common in the Mediterranean area (Civitelli & Brandano 2005), in the Indo-Pacific and in the Caribbean (Braga et al. 2010). They are a rich archive of past climatic and environmental information with a potential that is still underexplored (D'Atri 1990; Carannante et al. 1996; Basso & Tomaselli 1994; Basso et al. 1998; Pomar et al. 2002; Brandano et al. 2005; Civitelli & Brandano 2005; Halfar and Mutti 2005; Vigorito et al. 2005; Bassi et al. 2006; Bassi et al. 2010; Brandano et al. 2007; Brandano et al. 2009; Brandano et al. 2010; Brandano et al. 2012; Checchoni & Monaco 2008; Checconi et al. 2010; Braga et al. 2010; Puga-Bernabéu et al. 2010). They are also important hydrocarbon reservoirs with large oil and gas fields located in the Pacific and in the Atlantic areas (Erlich et al. 1990; Heubeck et al. 2004;

1 University of Milano-Bicocca, Dept. of Earth and Environmental Sciences, Piazza della Scienza 4, 20126, Milano, Italy. E-mail: g.coletti@campus.unimib.it; daniela.basso@unimib.it; cesare.corselli@unimib.it.
* Corresponding author.
2 Via Bramante 3, 20098, San Giuliano Milanese, Italy. E-mail: alfredo.frixa@alice.it.

Neuhaus et al. 2004; Sattler et al. 2004; Vahrenkamp et al. 2004; Fournier & Borgomano 2007; Borromeo et al. 2011; Coletti et al. 2015).

Unlike chlorozoan carbonate factories, rhodalgal factories may develop outside the tropical belt and in conditions (e.g., tropical upwelling regions) where hermatipic coral growth is inhibited and the platform lacks a marginal rim (Schlager 2003; Vigorito et al. 2005). Without this barrier to waves and currents, sediment transport and reworking may play an important role in the depositional architecture, and the platform often develops a ramp or a distally steepened ramp profile (Carannante et al. 1996; Pomar et al. 2002; Vigorito et al. 2005; Pomar & Kendall 2007; Williams et al. 2011). Similar processes of transport and resedimentation are also recorded in other carbonate systems dominated by loose-grained production (e.g., Senonian rudist-bearing platforms, Carannante et al. 1999; and Cenozoic foraminifer-dominated ramps, Beavington et al. 2005). Sediments transported basinward may have a high preservation potential (Parson-Hubbard et al. 1999; Halfar et al. 2001); if the carbonate factory become lost or unobservable, the transported skeletal remains might provide information on the shallow-water environment where they were produced (Nebelsick et al. 2001; Rasser & Nebelsick 2003). Therefore, when transport processes do not excessively alter the original composition of the sediment through mixing and selection, displaced materials can potentially be used to reconstruct the "lost" shallow-water environment (Nebelsick et al. 2001; Basso et al. 2012; Leszczyński et al. 2012). This could be especially useful in active, compressional tectonic settings, where short-lived small carbonate platforms develop on topographically high areas over thrust sheets and where resedimentation is frequent (Carannante et al. 1996; Bosence 2005).

Rhodoliths have an added value for these paleoecological reconstructions. During their growth, they bind skeletal grains of their native environment preserving the record of the changing benthic associations through time or space (Basso 1991; Basso & Tomaselli 1994; Basso et al. 1998; Checconi & Monaco 2008). Other organisms may also overgrow them or bore and nest inside (e.g., barnacles, bryozoans, encrusting foraminifers, mollusks, annelids, etc.) adding other fruitful details. These small and free-living "carbonate factories" can be regarded as "island habitats" (Lee et al. 1997) that retain all the information accumulated during their development and preserve them after transport and burial.

Geological setting and regional evolution

The Pietra da Cantoni Group develops from the Burdigalian to Early Langhian (Novaretti et al. 1995), and outcrops in the eastern sector of the Monferrato area (Piedmont, Italy), which is part of the TPB. The TPB is a long-lived basin that evolved from the Late Eocene to the Late Miocene over the inner part of the Alpine wedge and it has recorded the complex interplay between the tectonic forces of the continental collision. During the Early Oligocene, sedimentation in the TPB was confined to small fault-bounded basins and continental and shallow marine facies prevailed (Mosca et al. 2009; Rossi et al. 2009). In the Oligocene, the basin became deeper and there was a transition toward open marine conditions (Mosca et al. 2009; Rossi et al. 2009). At the beginning of the Miocene (Aquitanian stage), the deformation caused by the rotation of the Alpine Wedge (Maffione et al. 2008) uplifted and divided the Monferrato area into an eastern and a western sector. The western sector was deeper and dominated by a slope to basin environment as indicated by the deposition of siliceous ooze (Bonci et al. 1990; Clari et al. 1994; Clari et al. 1995; Novaretti et al. 1995). The eastern Monferrato was uplifted resulting in the formation of an angular unconformity along which the Aquitanian-Early Burdigalian interval is missing. In the Burdigalian the deformation was completed in the eastern Monferrato and the PDC deposited at the top of the unconformity developed upon the underlying deposits (Casale Monferrato, Marne di M. Piano, Cardona, Antognola Formations). In the western Monferrato basin instead, the sedimentation was dominated by siliciclastic sand.

During the Burdigalian the rhodalgal carbonate factories developed in a shallow sea environment, which was, according to paleogeographical reconstruction, between latitude 35° and 40° N (Meulenkamp et al. 2000). In the Early Miocene the Earth climate was globally warmer than present day, with tropical and subtropical climatic region extending to higher latitude (Adams et al. 1990; Billups et al. 2010). Reconstruction of the terrestrial climate of Europe, based on continental proxies, suggests temperatures up to 6°C warmer (Mosbrugger et al. 2005). Taking these elements into consideration a tropical climate is conceivable for the region, as testified by fossil assemblages (Vannucci et al. 1996). From the Langhian onward, the western and eastern Monferrato had similar subsidence rates, leading to uniform deposition of fine carbonate to mixed carbonate-siliciclastic sediments (the calcareous member of Tonengo sandstone Fm., Dela Pierre et al. 2003). After the Early Serravallian, a further deepening occurred, which is indicated by the deposition of the Marne di Mincengo Formation.

The PDC is divided into two sequences (Bicchi et al. 2006). The older Sequence 1 (Aquitanian-Lower Burdigalian) outcrops exclusively in the village of Rosignano Monferrato. It is composed of bioclastic wackestone

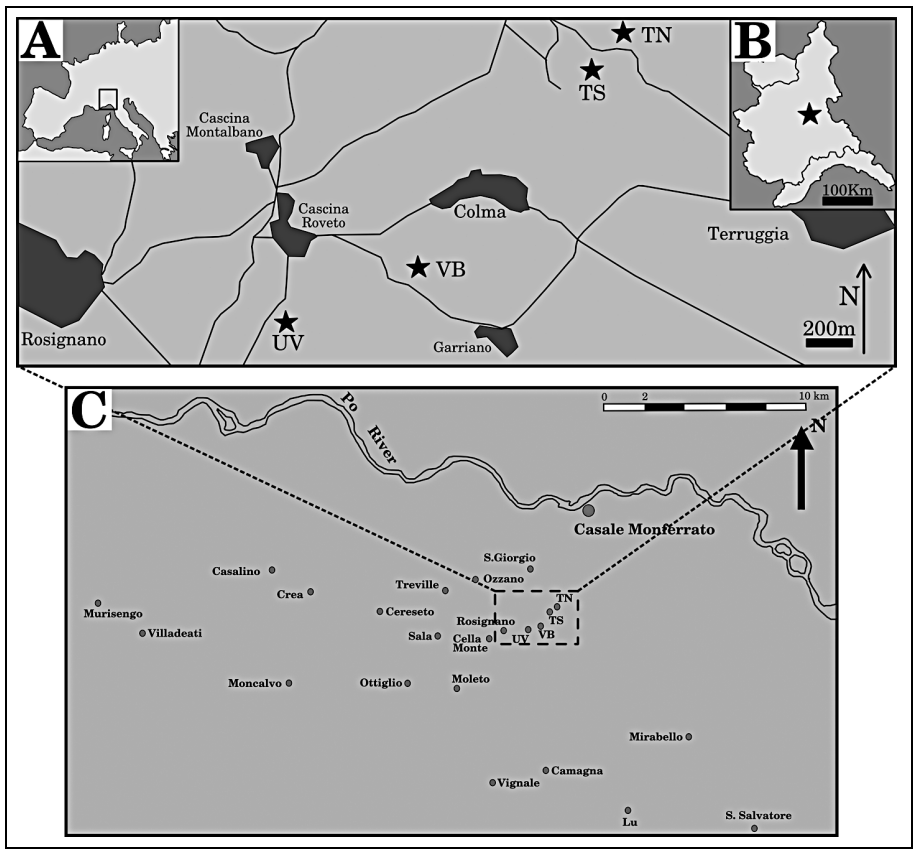

Fig. 1 - Upper panel: sketch map of the investigated outcrops (stars); Uviglie (UV; 45° 4.70' N 8° 24.79' E); Villa San Bartolomeo (VB; 45° 4.82' N 8° 25.27' E); Torre Veglio North (TN; 45° 5.53' N 8° 25.85' E); Torre Veglio South (TS; 45° 5.25' N 8° 25.84' E). A) Simplified map of Europe with Northwestern Italy (black box). B) Simplified map of Northwestern Italy, with the studied area (star). C) Map of all the outcrops of PDC, modified after Schüttenhelm, 1976.

and packstone with scattered rhodoliths. The boundary with the overlying Sequence 2 is a ravinement surface with small scattered lenses of rhodolith-rich, coarse bioclastic material (Bicchi et al. 2002). The second sequence is further divided into two units. The lower unit is the main subject of this work and outcrops only in the eastern part of the basin. It consists of coarse bioclastic limestone deposited in a shallow marine environment (Schüttenhelm 1976; Bicchi et al. 2006). The upper unit consists of marly packstones and marls deposited in a deeper environment (Schüttenhelm 1976; Bicchi et al. 2006). Outcrops of the upper unit of Sequence 2 are present in the whole PDC basin. The two units are separated by a thin interval that shows heavily reworked and bioeroded bioclasts (mainly mollusk shells but also small rhodoliths and fish bones), pebbles and authigenic minerals (mainly glaucony and phosphate). According to literature (Novaretti et al. 1995; Bicchi et al. 2006), the lower unit is referred to Biozone N7a (*Globigerinoides trilobus* subzone, Blow, 1969). The base of this biozone is marked by the disappearance of *Catapsydrax dissimilis* and dated at 17.62 Ma in the open ocean (Wade et al. 2011). In the TPB, an ash layer with an $^{40}Ar/^{39}Ar$ age of 18.7±0.2 Ma (Ruffini 1995; D'Atri et al. 1999; D'Atri et al. 2001), located above the disappearance of *Catapsydrax dissimilis*, suggests a possible diachrony of the event. On these bases, the lower unit of Sequence 2 should have been deposited between about 19 and 18 Ma (Novaretti et al. 1995). Calcareous nannofossils, planktonic foraminifers and miogypsinds distribution in the Villa San Bartolomeo succession shows that in the studied area, the lower unit of Sequence 2 belongs to Biozone N7a (Schüttenhelm 1976; Vannucci et al. 1996; Bicchi et al. 2002; Bicchi et al. 2006).

Materials and methods

Currently, the PDC outcrops are scattered and discontinuous. The rock is poorly cemented and porous, therefore it weathers rapidly and is generally covered by thick soil and dense vegetation. Outcrops are visible in villages and dismissed quarries. The lower unit of PDC Sequence 2 was studied in the following dismissed quarries located near the villages of Rosignano and Terruggia (Fig. 1): Villa San Bartolomeo (VB), Castello di Uviglie (UV), Torre Veglio North (TN), Torre Veglio South (TS). Presently, VB is no longer accessible and TN and TS are buried.

The outcropping successions were measured, and described by grain-size and texture. The rhodolith size was measured, and nodules larger than 3 cm were extracted and broken to study their internal structure and composition. The rhodolith shape and structure were described following Bosellini and Ginsburg (1971), Bosence (1983a) Vannucci et al. (1996) and Basso (1998).

Since VB, UV, TN and TS outcrops did not offer a sufficiently large surface for sedimentological observations of large-scale structures, further fieldwork was performed in the other nearby PDC outcrops. In particular, the outcrop of Rosignano, which is very close to the studied area (Fig. 1), offers a very large exposure of the lower unit of PDC

Sequence 2. Further observation were done in the Treville village, the westernmost outcrop of the rhodolith-bearing unit of PDC Sequence 2.

Thin sections of 115 samples collected by Vannucci et al. (1996) in VB and TN, and 85 samples collected in 2010 by the authors in UV and TS, were analyzed for this work. From these, 110 thin sections were obtained from isolated rhodoliths and 90 were dedicated to both rhodoliths and their embedding sediment. On 12 samples from UV and TS sections, X-ray diffraction (XRD; PANalytical's Xert PRO Materials Research Diffractometer) and X-Ray fluorescence (XRF; PANalytical's Eilon 3-XL energy dispersive X-ray fluorescence spectrometer) analyses were performed to assess their mineralogical and chemical composition after rhodolith removal. The glaucony of the samples was qualitatively studied following the procedure of Amorosi (1997) to assess its autochthony and its maturity.

The texture, composition and bioclastic assemblage of the rhodolith-embedding material were quantified by point counting (Flügel, 2009) on digital photomicrographs of thin sections. A 150x150 μm grid was used and an average of 400 points was counted in each analyzed section. The recognized categories were: coralline algae, barnacles, benthic foraminifers, planktonic foraminifers, mollusks, bryozoans, echinoids, serpulids, ostracods, micrite, sparite, glaucony, authigenic phosphate and non-carbonate minerals. On suitable thin sections of the rhodoliths, point counting was also performed on the sediment patches trapped within the nodules to assess the differences between the material inside and outside the rhodoliths. Data from point-counting were statistically treated by hierarchical cluster analysis and non-metric multidimensional scaling ordination (MDS) based on the Bray-Curtis similarity with PRIMER 6 (Kruskal 1977; Field et al. 1982; Clarke & Gorley 2006).

The growth-form and relative abundance of coralline algae were studied on thin sections. Coralline taxonomy follows Kato et al. (2011) and Bittner et al. (2011). The identification of foraminifers was conducted to the lowest taxonomic level possible (mostly genus or species), which required extraction of foraminifer tests from the sediment after disaggregation of rock samples. The foraminifers were identified under stereomicroscope and scanning electron microscope (SEM; TESCAN mega TS5136 XM). For SEM analysis, specimens were cleaned, mounted on SEM stubs by an adhesive conductive carbon disk and then gold-coated. With the exception of the SEM-prepared specimens, the remaining foraminifers were eventually embedded in epoxy resin, cut and prepared in thin sections. The taxonomic nomenclature follows Loeblich & Tappan's revision (1987). Among the other skeletal grains the most abundant taxa of barnacles, bryozoans and mollusks were also identified.

Results

The results have been divided in two sections, a former with the presentation of the detailed paleontological and sedimentological data of the four main outcrops (Villa San Bartolomeo, Uviglie, Torre Veglio North and Torre Veglio South) and a latter dedicated to the sedimentological description of Rosignano and Treville outcrops.

Villa San Bartolomeo (VB), Uviglie (UV), Torre Veglio North (TN) and Torre Veglio South (TS)

Paloeontological and sedimentological analyses in these outcrops allowed the recognition of different facies, lithozones and the identification of the most abundant taxa of the fossil association.

Facies description. Four facies were recognized, based on rock characteristics, texture, and statistical treatment of compositional data (Fig. 2). Each facies includes one or more lithozones, identified in the outcrop on the basis of their rock texture, mineralogy and macroscopic fossiliferous content. Lithozones were numbered from 1 to 6, from the oldest to the youngest (Tab. 1; Fig. 3).

Facies 1 is a typical rhodalgal assemblage (sensu Carannante et al. 1988) characterizing lithozones 1 to 4a. The coarse skeletal elements are composed of rhodoliths, large benthic foraminifers and barnacle plates. The fine fraction is dominated by fragments of coralline algae, barnacles, benthic foraminifers, bryozoans, echinoids and mollusks. In the hierarchical cluster analysis and MDS ordination, samples of Facies 1 gather in Clusters 1 and Cluster 2. The rock is an almost pure limestone with a siliciclastic fraction primarily composed of silt-sized and sand-sized grains of quartz.

Facies 2 characterizes the upper part of the fourth lithozone (4b). Large skeletal elements are rhodoliths and barnacle plates. The fine fraction is mainly composed of planktonic foraminifers and grains of authigenic minerals. The rock is an impure limestone: it is rich in silicate minerals constituting up to 40% of the fine-grained fraction. Samples of this facies are included in the Cluster 3.

Facies 3 characterizes lithozone 5. The coarse fraction of the rock is composed of abraded, winnowed and often phosphatized bioclasts (mainly pebble-size rhodoliths and mollusk shells). The finer material embedding the large elements is almost entirely composed of planktonic foraminifer tests, glaucony and authigenic phosphate grains. In the hierarchical cluster analysis and MDS ordination the samples of Facies 3 and 4 are grouped in Cluster 4. The rock is a marly limestone, and nearly half of the material is composed of silicate minerals.

Facies 4 characterizes lithozone 6. Large skeletal elements are almost absent, and most of the rock is composed of planktonic foraminifer tests; glaucony grains are frequent and phosphate grains occur. The rock is a marly limestone with abundant clay minerals. In the hierarchical cluster analysis and MDS ordination the samples of this facies are encompassed in Cluster 4, together with Facies 3.

Lithozones description. In the outcrops on the basis of their rock texture, mineralogy and macroscopic fossiliferous content different lithozones were identified. The lithozones were numbered from 1 to 6, from the oldest to the youngest (Fig. 3), their characteristics are summarized in Table 1. The thickness and characteristics of the lithozones slightly vary among the quarries, and certain lithozones do not occur in all quarries.

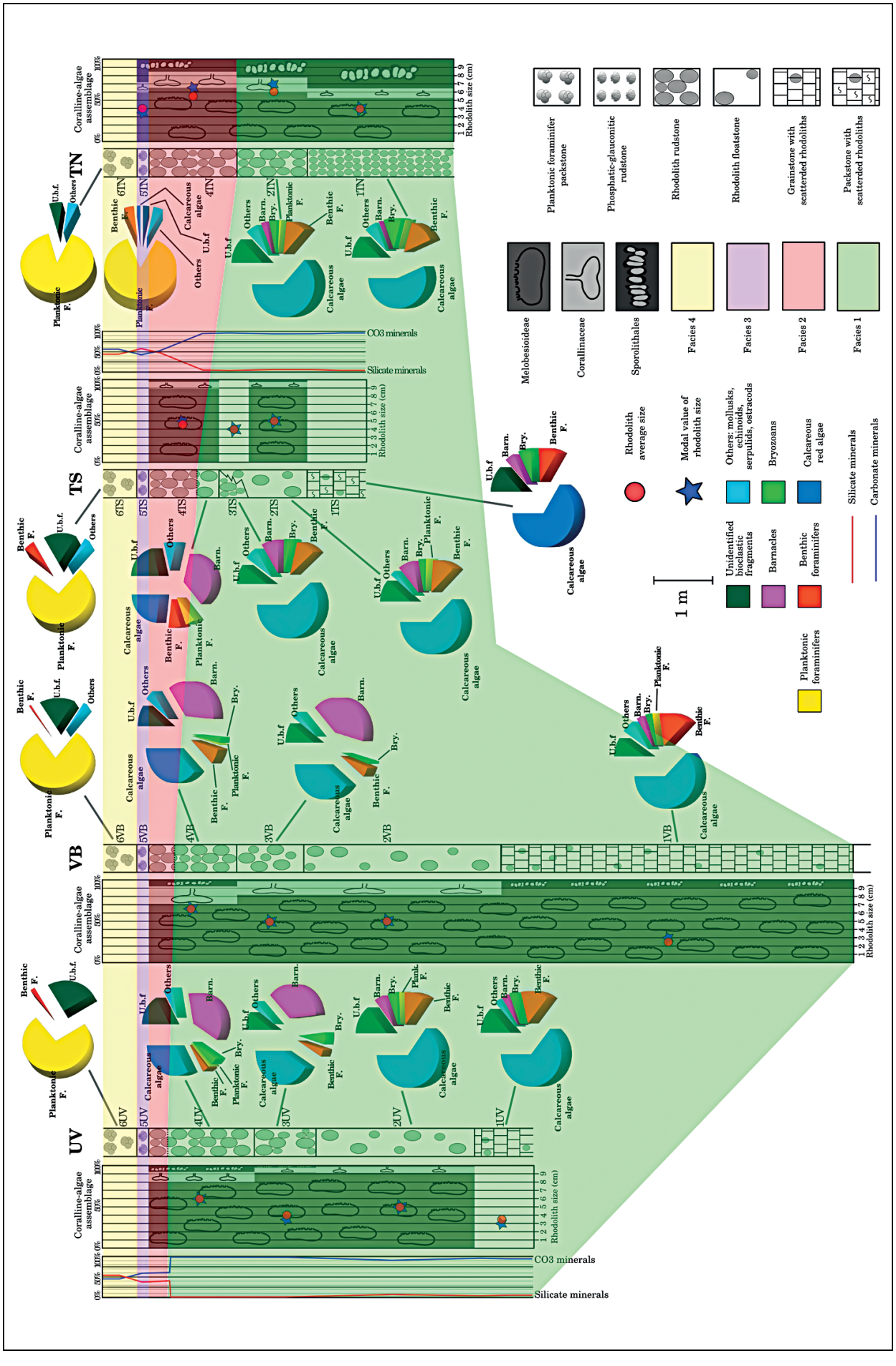

Fig. 2 - Simplified stratigraphic log of the studied PDC sections summarizing bioclastic composition, mineralogical composition, general attributes of sampled rhodoliths, coralline-algae assemblages and facies distribution. In lithozones 1UV, 1TS, 3TS, coralline algae were insufficiently studied due to poor preservation.

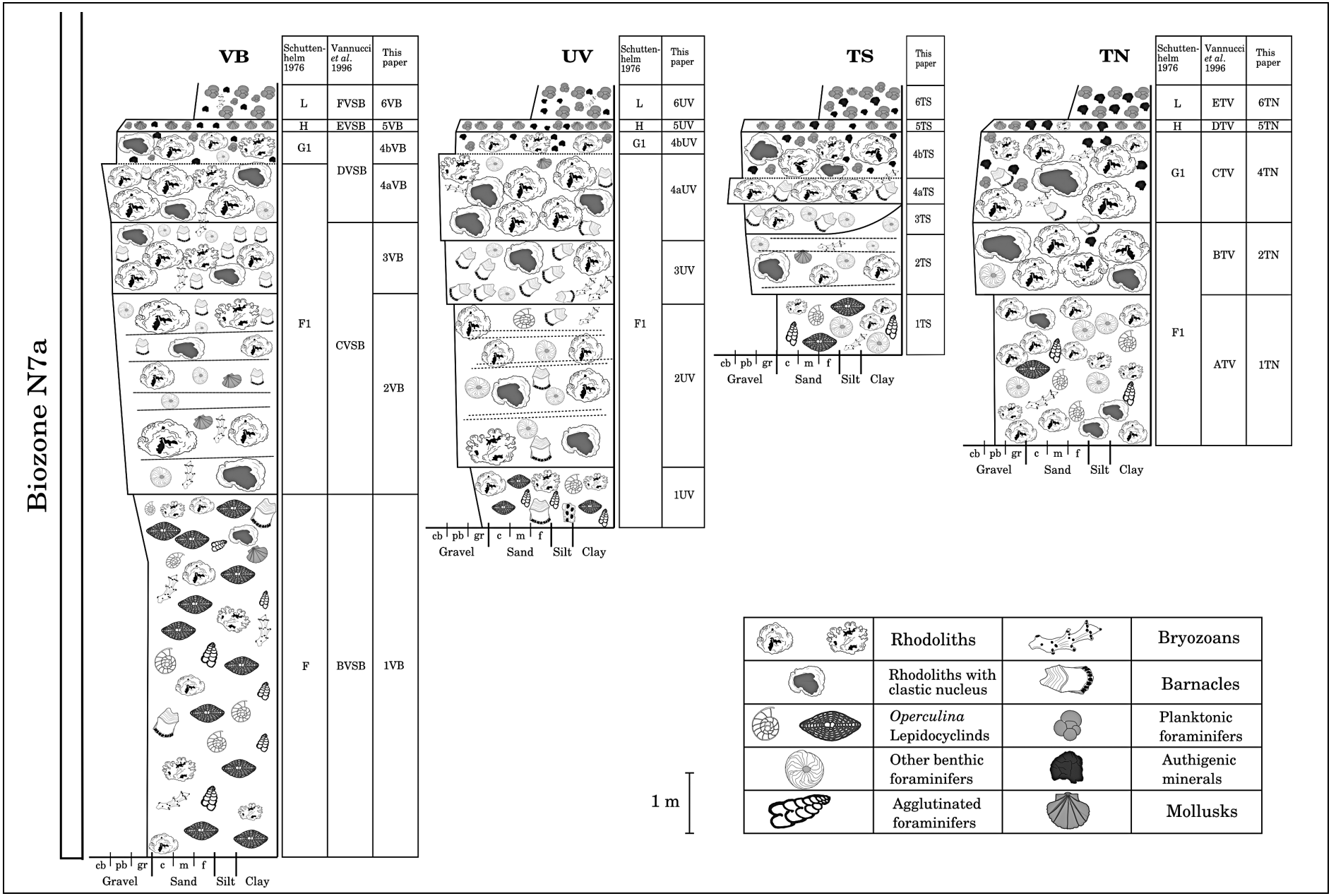

Fig. 3 - Stratigraphic log of the studied sections in PDC and comparison with previous works; f: fine; m: medium; c: coarse; gr: gravel; pb: pebble; cb: cobble; Biozone N7a according to Blow (1969).

Tab. 1 - Lithozone characteristics.

UV		VB		TS		TN	
6	Glauconitic, planktonic foraminifers marly-packstone. Micrite is abundant	6	Glauconitic, planktonic foraminifers marly-packstone. Micrite is abundant	6	Glauconitic, planktonic foraminifers marly-packstone. Micrite is abundant	6	Glauconitic, planktonic foraminifers marly-packstone. Micrite is abundant
5	Phosphatic-glauconitic rudstone. Micrite is abundant	5	Phosphatic-glauconitic rudstone. Micrite is abundant	5	Phosphatic-glauconitic rudstone. Micrite is abundant	5	Phosphatic-glauconitic rudstone. Micrite is abundant
4b	Glauconitic rhodolith rudstone. Micrite is present	4b	Glauconitic rhodolith rudstone. Micrite is present	4b	Glauconitic rhodolith rudstone. Micrite is present	4b	Glauconitic, reverse graded, rhodolith rudstone. Micrite is present
4a	Rhodolith rudstone. Without interstitial material	4a	Rhodolith rudstone. Without interstitial material	4a	Rhodolith rudstone. Without interstitial material	4a	Absent
3	Barnacle and rhodolith rudstone. Without interstitial material	3	Barnacle and rhodolith rudstone. Without interstitial material	3	Rhodolith rudstone with barnacle fragments. Without interstitial material	3	Absent
2	Bedded rhodolith floatstone. Almost without interstitial material	2	Bedded rhodolith floatstone. Almost without interstitial material	2	Bedded rhodolith floatstone. Almost without interstitial material	2	Rhodolith rudstone. Almost without interstitial material
1	Lepidocyclinid grainstone with scattered rhodoliths. Without interstitial material	1	Lepidocyclinid grainstone with scattered rhodoliths. Without interstitial material	1	Coralline-algae packstone with scattered rhodoliths. Micrite is abundant	1	Rhodolith rudstone. Micrite is abundant

These lithozones can be correlated with those used by previous authors (Fig. 3).

1VB, the basal lithozone of the VB section, is a lepidocyclinid-rich grainstone with scattered small rhodoliths. The rock is characterized by a weak fabric with common orientation of the large and flat skeletal elements. This lithozone is overlain by a bedded rhodolith floatstone (2VB), which is then followed by a rudstone composed of barnacle fragments and rhodoliths (3VB). The fourth lithozone (4VB) is a rhodolith rudstone. The material in which the rhodoliths are embedded at the base is composed of coarse skeletal fragments (mainly barnacle and coralline debris) (4aVB), whereas at the top is mainly composed of planktonic foraminifers and grains of glaucony and phosphate (4bVB).

The base of the UV succession (Fig. 4A), 1UV, is a lepidocyclind-rich grainstone, with scattered small rhodoliths. The overlying 2UV lithozone is composed of several 30-50 cm thick beds of rhodolith floatstone alternated with thin beds of coralline-rich grainstone (Fig. 4A, C). The thickness of these beds is variable and most of them are laterally discontinuous. In the upper part of this lithozone, near the boundary with the overlaying 3UV lithozone, small, lens-shaped bodies of rhodolith floatstone are present (Fig. 4D). The boundary between 2UV and the overlaying 3UV is sharp and probably erosional (Fig. 4C). 3UV is a rudstone composed of barnacle debris and rhodoliths. The base of the lithozone is rich in rhodoliths while upward they are less common. The rock presents a weak fabric with a common orientation of the large and flat skeletal elements. The lithozone 4UV is a rhodolith rudstone that is rich in bioclastic fragments at the base (4aUV) and in planktonic foraminifers, glaucony and phosphate grains at the top (4bUV).

1TS, the first lithozone of the TS succession (Fig. 4B), is a rhodolith packstone. 2TS is a bedded rhodolith floatstone, alike 2UV. The 3TS is a laterally discontinuous rhodolith rudstone rich in barnacle debris. The lithozone 4TS, similarly to 4VB and 4UV, is subdivided in two part: 4aTS and 4bTS.

The basal lithozones of TN, 1TN and 2TN are massive rhodolith rudstone (in 2TN rhodoliths are larger than in 1TN).

The TN quarry lacks a lithozone characterized by barnacle abundance and without glaucony and phosphate grains (the lithozone 3 of the other quarries). The lithozone 4TN is a rhodolith rudstone. Since rhodolith-embedding material in 4TN, from the base to the top, is principally composed by planktonic foraminifers, glaucony and phosphate grains, the whole lithozone was correlated with the upper part of the fourth lithozone (4b) of the other quarries.

Lithozones 5 and 6 have the same characteristics in all of the studied quarries (Tab. 1; Fig. 3). The lithozone 5 (lag deposit) is a thin bed of winnowed, phosphatized and glauconized material, mollusk shells, small rhodoliths, fish skeletal remains and rock fragments from the Casale Monferrato Fm. This lithozone is easily recognizable and separates the lower and the upper units of Sequence 2. It belongs to the uppermost part of Biozone N7a (Bicchi et al. 2006). The lithozone 6 is a planktonic-foraminifers-rich marly packstone; this lithozone is the base of the upper unit of Sequence 2.

From a chemical and mineralogical perspective, lithozones 1 to 4a are almost pure limestone (90-98% carbonate minerals) while 5 and 6 are marly limestone (60% carbonate minerals; Fig. 2). The 4b is an impure limestone because the rhodolith embedding material is mainly composed of authigenic minerals and clays (Fig. 2). Calcite has a low magnesium content (Mg/Ca0,01);

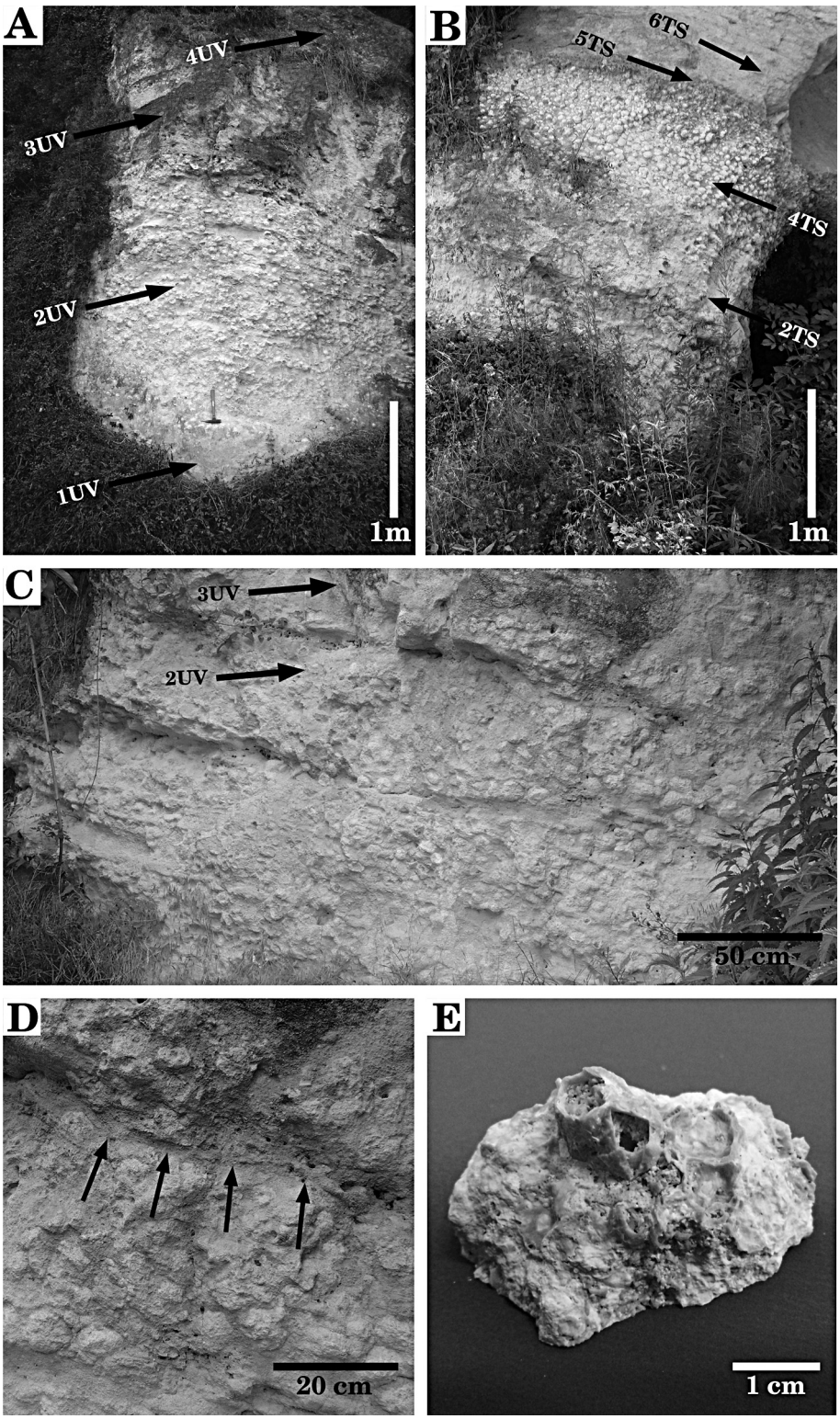

Fig. 4 - Field pictures of the studied successions. A) Lithozones from 1 to 4 of UV quarry. B) Lithozones from 2 to 6 of TS quarry. C) Lithozone 2UV structures and the lower part of the overlaying lithozone 3UV. D) Lens of rhodolith floatstone at the boundary between lithozone 2UV and lithozone 3UV; arrows = base of the lens. E) Barnacle encrusting rhodolith surface.

quartz is the most common silicate mineral found in lithozones 1 to 4a, while clay minerals become abundant upward.

The phosphorous concentration increases and phosphatized bioclasts become more frequent from part b of the lithozone 4 upward. Glaucony is present in the whole succession. In lithozones 1, 2, 3 and 4a, glaucony is rare and is mainly present as the filling of skeletal-grain porosity; the grains are small, without cracks and of a pale-green color. Upward it is common and especially abundant in lithozones 5 and 6. In the latter lithozones the glaucony grains are larger and of a deep-green color, they also present cracks filled with pale-green glaucony (Fig. 5A, B). The angular shape of the grains and their occurrence as the filling of intraparticle porosities, suggest an *in situ* origin for these minerals in all

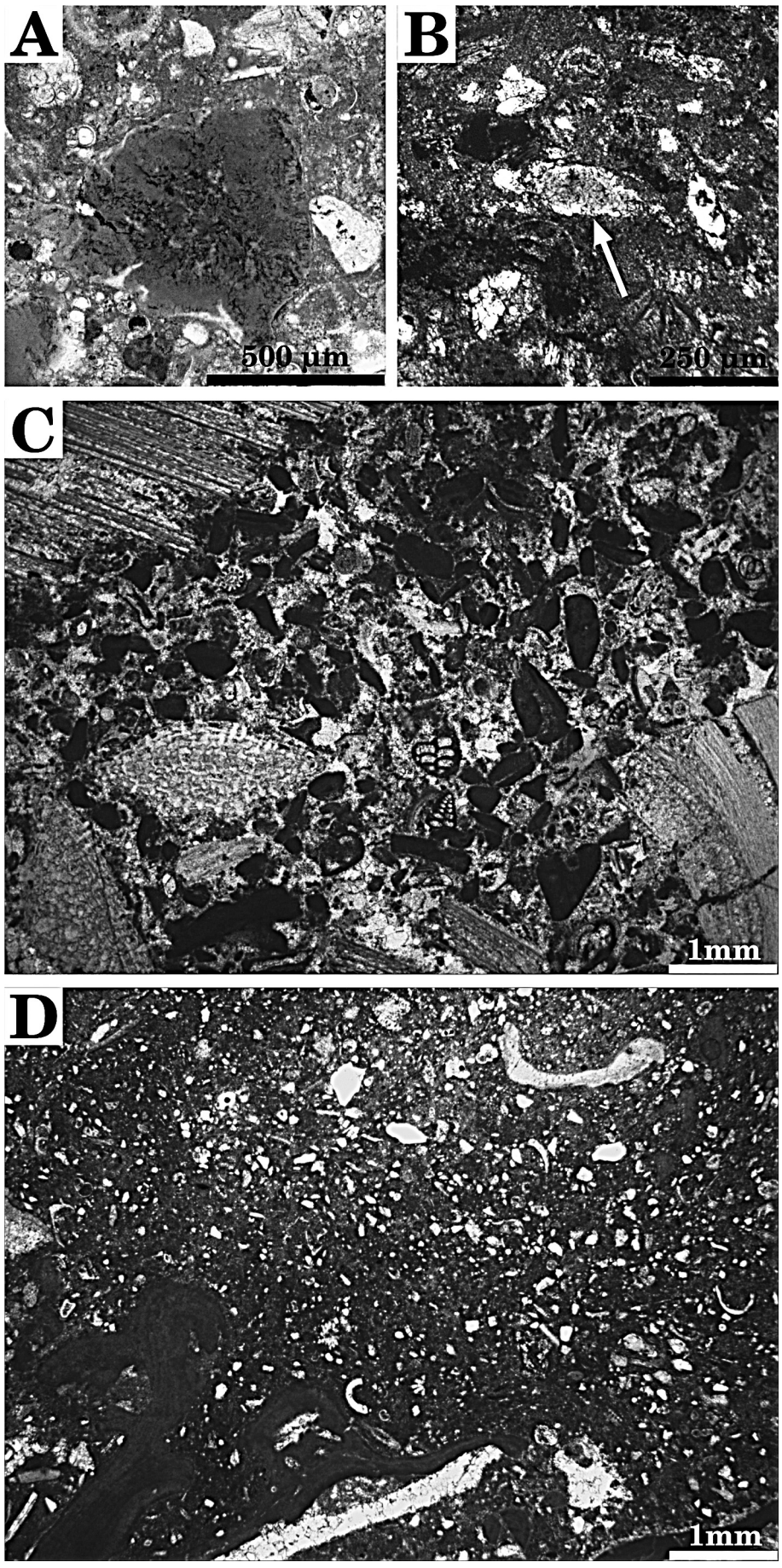

Fig. 5 - Glaucony grains. A) Highly mature glauconite. B) Glaucony grain with an average degree of maturity (arrow). C) Shallow-water skeletal grains inside the rhodolith from Treville outcrop. D) Deeper water sediment outside the same rhodolith from Treville outcrop.

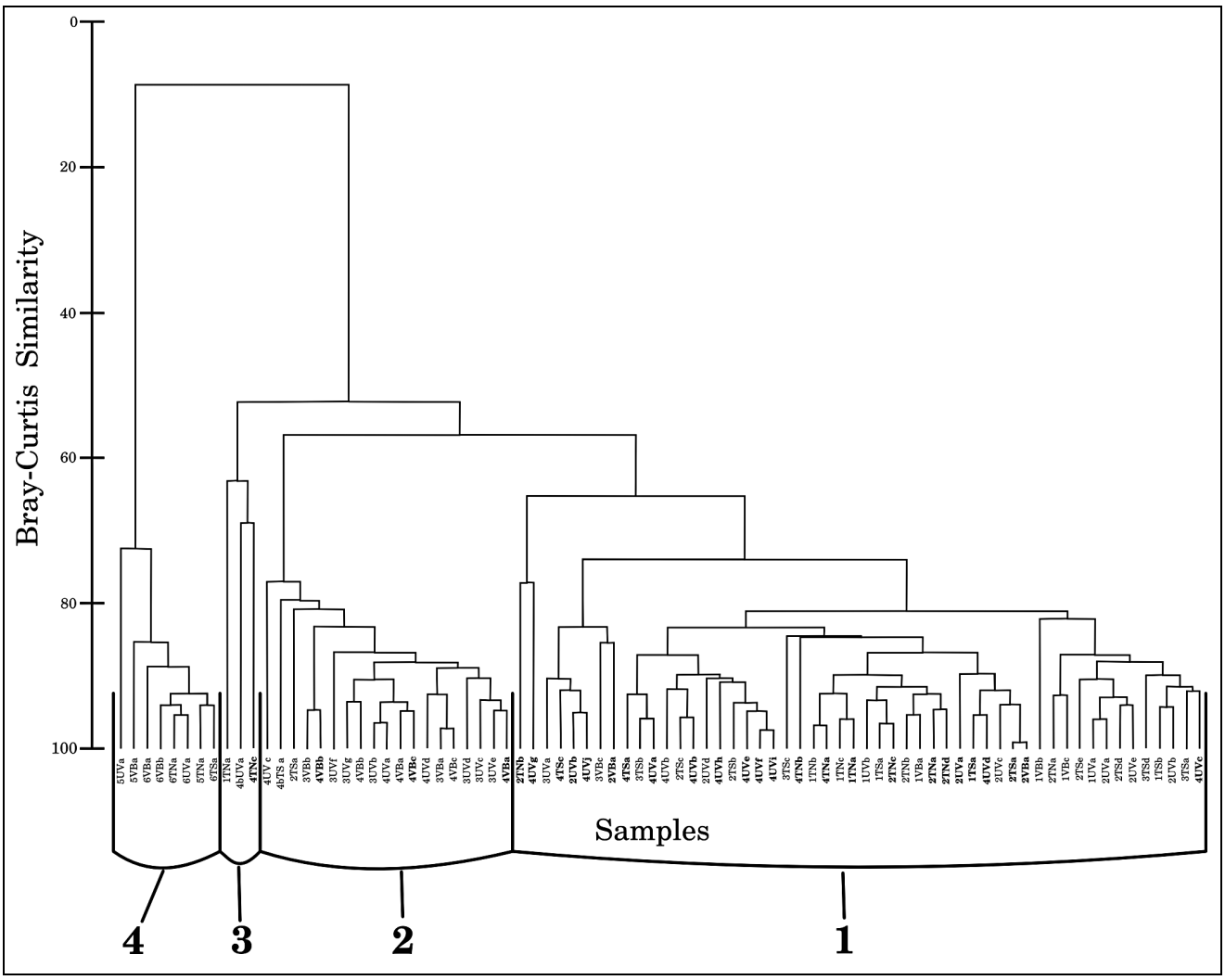

Fig. 6 - Hierarchical agglomerative dendrogram based on Bray-Curtis similarity of the bioclastic composition of samples. Point counts of bioclastic composition were standardized and then analyzed for Bray-Curtis similarity. The samples are grouped in clusters 1 to 4 at 60% of Bray-Curtis similarity. Samples from inside rhodoliths are in bold.

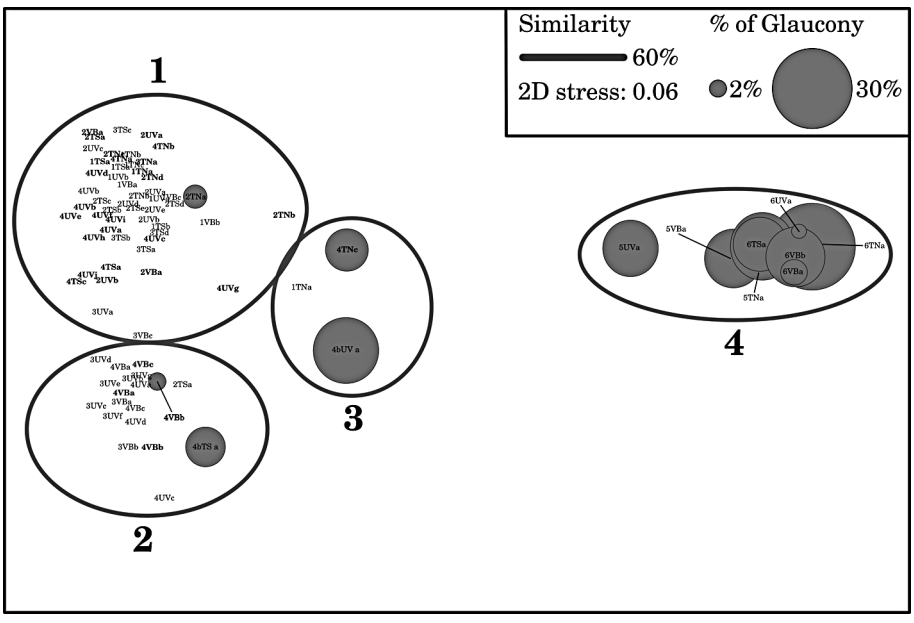

Fig. 7 - MDS (2D) ordination of the samples, based on the same Bray-Curtis similarity as Figure 6. 2D stress indicates the displacement of the sample in the representation from its actual position in the multidimensional space. Circles represent the amount of glaucony in samples, with circle radius proportional to glaucony abundance.

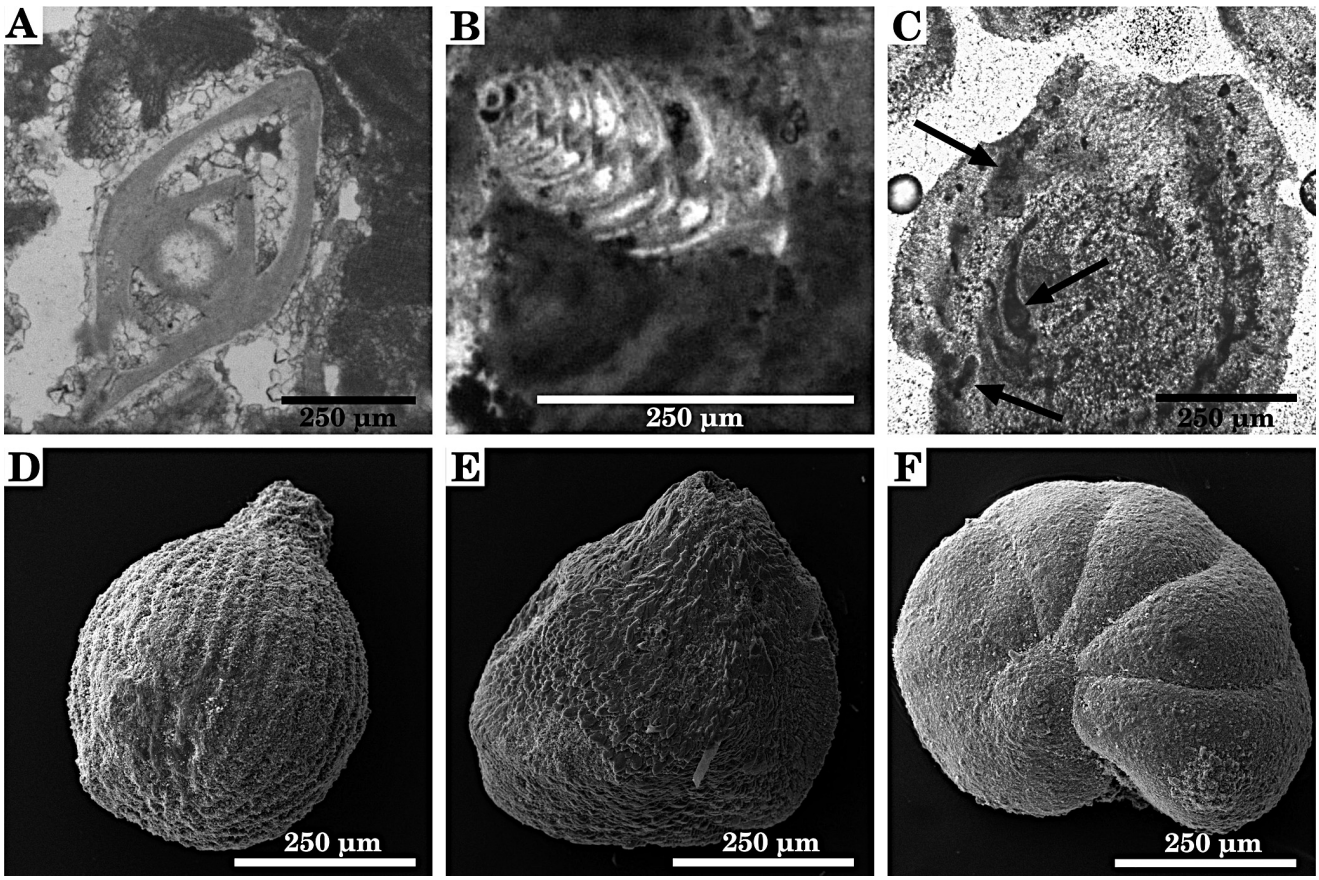

Fig. 8 - Microfossils. A) *Lenticulina* B) Bolivinidae sp. C) *Amphistegina* with chambers filled by glaucony; arrows = glaucony. D) *Lagena* E) *Bifissurinella lindenbergi*. F) *Lobatula lobatula*.

the lithozones. The abundance of authigenic minerals peaks in lithozone 5.

Multivariate Statistical Analyses. Data from point-counting analyses of biogenic components, performed on both the material inside and outside of the rhodoliths, were classified by a hierarchical cluster analysis and ordinated by non-metric multidimensional scaling (MDS). This procedure identified three large groups and a smaller group at 60% of Bray-Curtis similarity (Figs 6, 7). Clusters 1 and 2 include all of the samples from Facies 1 (lithozones from 1 to 4a), including also samples from inside the rhodoliths. Cluster 1 encompasses samples rich in coralline algae debris and benthic foraminifers, whereas samples with abundant barnacle fragments are in Cluster 2.

The small Cluster 3 stands in the central part of the plot, slightly closer to Cluster 1 and 2; this cluster includes samples from Facies 2 (lithozone 4b) together with samples with peculiar assemblages. In sample 1TNa, bryozoans are more abundant than in any other sample, whereas in samples 4TNc (a bioturbation of the outer layer of a rhodolith) and 4bUVa, coralline algae and barnacle fragments are mixed with planktonic foraminifers.

Cluster 4 includes all of the samples from Facies 3 and 4 (lithozones 5 and 6).

Glaucony is far more abundant in Clusters 4 and 3 than in Clusters 1 and 2 (Figs 6-7).

Rhodoliths. According to pebble shape classification (Zingg 1935; adopted for the algal nodules by Bosence 1983a), most of the studied rhodoliths are spherical, discoidal specimens are rare. This result is confirmed by the quantitative sphericity analysis (Sneed & Folk 1958): most rhodoliths have sphericity > 0.8. Rhodoliths are small, pebble-sized (long axis less than 6.5 cm) in lithozone 1 and generally large, cobble-sized (long axis more than 6.5 cm) from lithozone 2 upward (Fig. 2).

The coralline growth form is almost always encrusting to lumpy and has an internal laminar structure made of closely stacked overgrowing crusts. Some rhodoliths with a columnar structure have been observed in 5TN.

Melobesioideae dominate the rhodolith algal assemblages, with abundance ranging from 60% to 90% (Fig. 2). Corallinaceae and Sporolithales are common accessories. Among Corallinaceae, *Spongites* and *Lithoporella* are the most frequent genera. Lithophylloideae are rare and were only identified in 4VB, 4UV and 5TN. The most abundant species are *Lithothamnion moretii*, *Lithothaminion gianmarinoi*, *Lithothamnion* sp., *Phymatholiton* sp., *Mesophyllum roveretoi*, *Sporolithon* sp., *Spongites fruticulosus* and *Lithoporella melobesioides.*

Rhodolith nucleus is generally composed of bioclastic material. Some nodules grow as coated grains (Steneck 1986; Basso et al. 2009) around large angular to sub-angular pebbles issued from the Casale Monferrato Fm.

In Facies 1, the bioclastic debris trapped inside the rhodoliths is composed of coralline fragments (50-70%), barnacle detritus (10-30%), benthic foraminifers (5-10%) and rare fragments of mollusks, bryozoans, echinoids and serpulids. The same association of skeletal grains is also observed in all of the boreholes of the algal nodules. In Facies 2, the very same association of skeletal grains is observed trapped inside the rhodoliths, whereas, planktonic foraminifers and glaucony grains are found in the boreholes of the outer layer of the rhodoliths. Rhodolith surfaces are often encrusted by bryozoans, barnacles (Fig. 4E) and serpulids; rhodoliths with barnacle-encrusted surfaces are especially common in lithozones 3 and 4.

Other skeletal grains: distribution and preservation. Coralline fragments are the main component of the studied lower unit of Sequence 2 (Facies 1 and Facies 2; lithozones 1 to 4); in lithozones 1 and 2 they represent up to 60%-65% of the skeletal grains. In the lithozones 3 and 4a, in the UV and VB quarries, the percentage of coralline algae debris is lower (30-40%) and barnacle fragments are more abundant (40%). Entire individual barnacles encrusting the rhodoliths have been observed in lithozones 2, 3 and 4 (Fig. 4E). The studied specimens have been identified as *Balanus* sp. and placed in the *Balanus trigonus* group (sensu Newman & Ross 1976) on the basis of their similarity to *B. spongicola* and *B. calidus* (Buckeridge pers. comm., 2013).

Benthic foraminifers are generally common (10%) but in the lithozones 3 and 4, in the UV and VB quarries, they are scarce. Textulariidae comprise 20-25% of the total observed benthic foraminifers in lithozone 1, their numbers decrease upward. In VB and UV quarries, in lithozone 1, large lepidocyclinids (*Nephrolepidina tourneri* and *Eulepidina dilatata* according to Schüttenhelm 1976) dominate the association. In lithozone 2, 3 and 4, and in lithozone 1 in the TN and TS quarries, the association is dominated by *Lobatula lobatula* (Fig. 8F), *Amphistegina* cf. *radiata* (identified following O'Herne 1974 description) and *Elphidium crispum*. *Operculina complanata*, *Miogypsina* spp., *Rosalina* sp., *Eponides repandus*, *Sphaerogypsina globulus*, *Stomatorbina torrei* and *Neoconorbina orbicularis* are common accessories.

In Facies 1 and Facies 2, specimens of *Lenticulina calcar*, *Lagena* and Bolivinidae (Figs 8A, D, B) were found in association with the previously mentioned shallow-water foraminifers despite their typical distribution in deeper waters.

Planktonic foraminifers are uncommon in Facies 1, they become more frequent in Facies 2 and they are extremely abundant in Facies 3 and Facies 4. Among them, *Globigerina ciperoensis*, *Globigerina praebulloides*, *Globigerinoides trilobus*, *Globigerinoides quadrilobatulus*, *Zeaglobigerina woodi woodi* and *Globaquadrina dehiscens* are common species (Bicchi et al. 2006).

Bryozoans are present as minor components and are slightly more frequent in TN and TS than in the VB and UV quarries. In Facies 1 and Facies 2, the articulated bryozoan of the Bicorniferidae family, *Bifissurinella lindenbergi* (Fig. 8E) commonly occurs. Mollusks and echinoids are less frequent than bryozoans, except in Facies 3 where bivalve shells are abundant. Bivalve identification is hindered by poor preservation, and whenever complete specimens are found (generally large *Pecten*), the shells are too brittle for extraction; no articulated specimens were observed. Specimens of the genera *Pecten*, *Flabellipecten*, *Amussium*, *Cardita*, and *Ostrea* have been recognized. Serpulids and ostracods are rare. Deep-water ostracods have been reported by previous authors (Schüttenhelm 1976). Gastropods were not directly observed but gastropod borings were observed on barnacle shells.

Breakage and abrasion are the most common biostratinomic processes observed on skeletal grains; rounding is negligible, and most of the bioclasts retain their angular shape. Barnacle opercular plates are thinned, and their superficial features are abraded. Parietal plates are highly fragmented and abraded, and only their upper and thicker edges are usually preserved. In lithozones 2 to 4, *Amphistegina* tests are frequently eroded and the innermost whorl of the chamber can be exposed; *Elphidium* and lepidocyclinid tests are also often deeply abraded. Bivalve shells are generally fragmented. Borings are common in rhodoliths, and gastropod perforations are frequent on barnacle opercular plates. Encrusting bryozoans, although not abundant, are scattered on barnacle plates and coralline algae; coralline algae encrust both barnacle plates and bryozoan colonies. Rare and poorly preserved specimens of *Amphistegina*, *Lepidocyclina* and *Miogypsina* with chamberlets filled by glaucony are present in lithozones 2 to 4 (Fig. 8C). Bryozoan zoecia and other skeletal porosities in Facies 1 are also infrequently filled by glaucony. Phosphatization and glaucony fillings of skeletal grains are common in Facies 3.

Rosignano and Treville

Rosignano outcrop dominates the top of the hill where the village was built. It is long several hundreds of meters and over 15 meters high. The base of the succession is massive (Fig. 9A); the central and upper portions are bedded, with each bed 2 to 20 cm thick, frequently showing an erosive base (Fig. 9C). In the

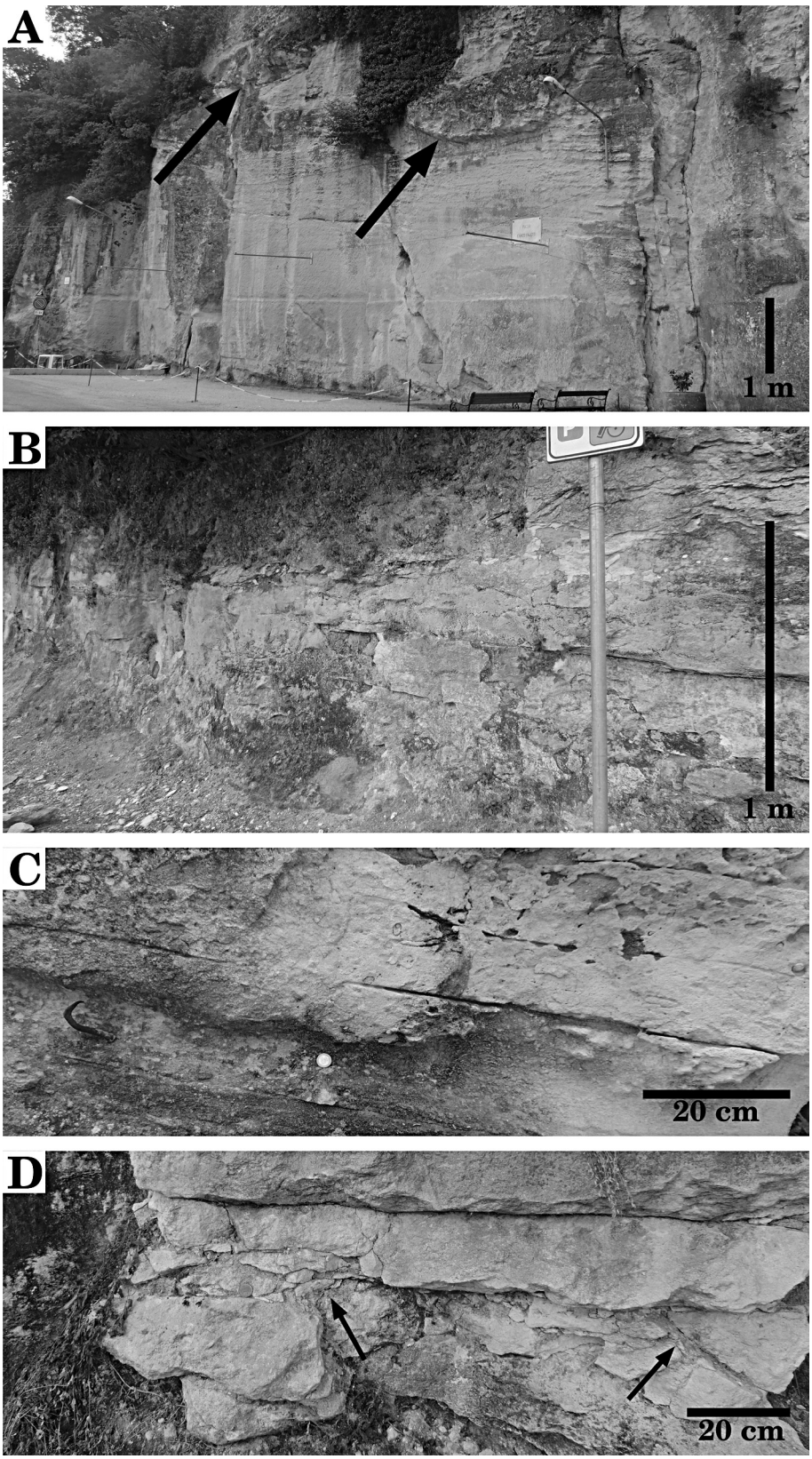

Fig. 9 - Rosignano outcrop (45° 4.85' N 8° 24' E). A) Overview of the outcrop; arrows=channels. B) Western part of the outcrop. C) Lens shaped bodies in the western part of the outcrop. D) Detail of the erosive base of the beds.

upper part of the outcrop, several channels are present (Figs 9A, 10A, B). In the western part of the outcrop the succession is thinner and bedded, with beds 5 to 40 cm thick (Fig. 9B). Thick beds are continuous while thin beds are composed by small lens-shaped bodies cutting each other (Fig. 9D). Cut samples show a weak fabric of the bioclasts. Small mud-clasts are abundant. The rock is a grainstone with large benthic foraminifers, echinoderm plates, bryozan colonies and scattered rhodoliths. Rhodoliths are abundant just in the upper-

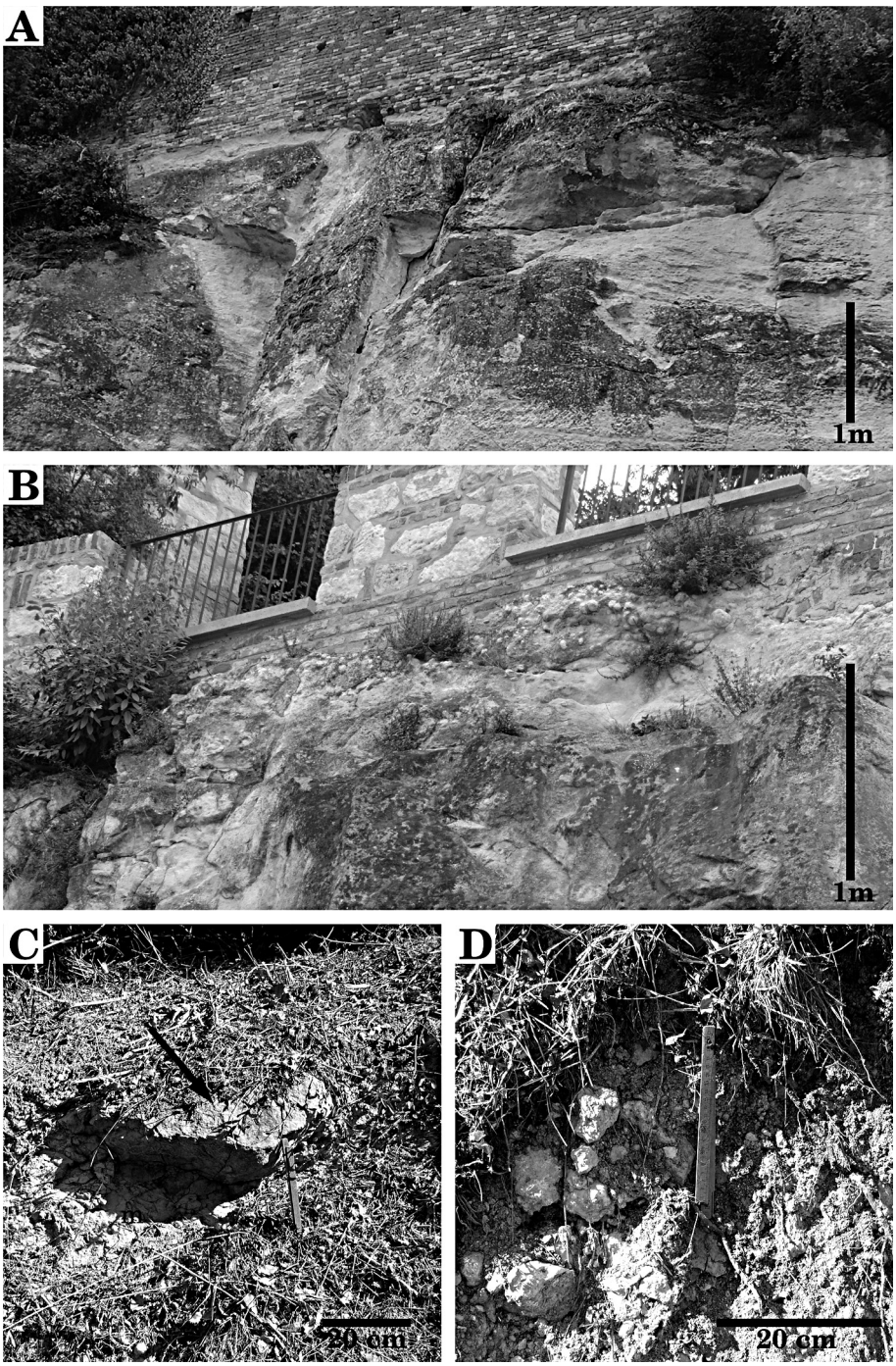

Fig. 10 - A) Detail of a large channel in Rosignano outcrop. B) Detail of a rhodolith-filled channel in Rosignano outrcop. C) Coarse bioclastic limestone (arrow) interbedded in marls (m), in Treville outcrop (45° 5.81' N 8° 22' E). D) Rhodoliths scattered within the marls in Treville outcrop.

most part of the succession, in a channel deposit (Fig. 10B).

Treville outcrop is located on the hill of the village graveyard, and consists of marls interbedded with skeletal grainstone (Fig. 10C). Rhodoliths-rich beds are also present (Fig. 10D). The skeletal assemblage observed within the rhodoliths of these beds is composed by coarse, shallow-water, skeletal fragments (Fig. 5C). The marls in which the rhodoliths are embedded are mainly composed of clay, micrite and tests of planktonic foraminifers (Fig. 5D). Both Treville and Rosignano outcrops belongs to biozone N7a (Schüttenhelm 1976; Bicchi et al. 2006).

Discussion

The Burdigalian PDC Platform

Several sedimentological and paleontological evidences suggest that the carbonate sediment of the lower unit of PDC Sequence 2 moved from their shallow-water original environment toward slightly deeper waters.

1. The coarse skeletal layers, interbedded in marls in Treville, were also deposited by sediment gravity-flows, but in a deeper environment, probably on the slope of the platform. According to a previous reconstruction of the basin (Schüttenhelm 1976) Treville was

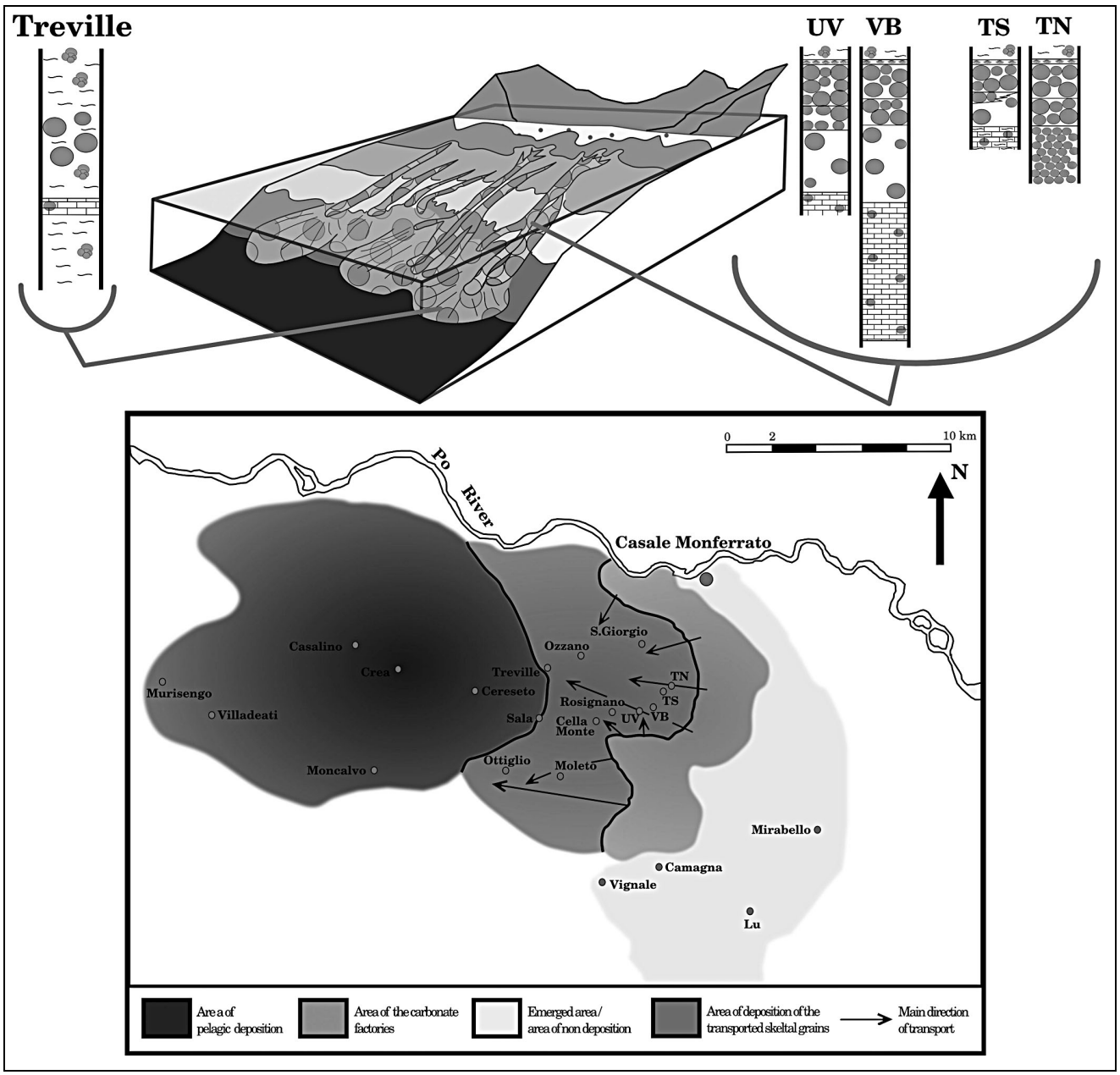

Fig. 11 - Reconstruction of PDC basin during the deposition of Sequence 2, lower unit. The position of the main localities of PDC and the depositional environments of the carbonate ramp are shown. Modified after Schüttenhelm (1976).

closer than UV, VB, TN, TS and Rosignano to the basin depocenter (Fig. 11). Being the westernmost outcrop of coarse skeletal limestone, it represents the distal margin of a submarine deposit formed by skeletal grains that were produced by the shallow-water rhodalgal carbonate factory of the PDC platform (Fig. 11).

2. The channels and the erosional scars in the Rosignano outcrop suggest that the sediment was probably transported by sediment gravity-flow. The common presence of mud clasts and the lack of a strong fabric support this interpretation (Major 1998; Mutti et al. 2009). These events may have been triggered by the impact of storm currents. Strong currents generated by storm waves can provide enough energy to trigger sediment motion (Paull et al. 2003). Each channel scour probably represents a single event in which the sediment gravity-flow erodes the underlying substrate and then fill the depression. The presence of a rhodolith-filled channel at the top of Rosignano succession is an evidence that flows, mainly composed by rhodoliths, were common in the PDC platform (Fig. 10B). The beds in the western part of Rosignano outcrop (Figs 10B, D) were also deposited by gravity-flows. The nearby VB, UV, TN and TS deposits probably originated in a similar way, as suggested by the presence of lensoidal beds (Fig. 4C, D). However, due to the small exposed surface, it was impossible to observe any large-scale structure.

3. No fossil in life position was observed in the studied outcrops. Bivalve shells and colonies of articulated bryozoans (*Bifissurinella lindenbergi*) were always

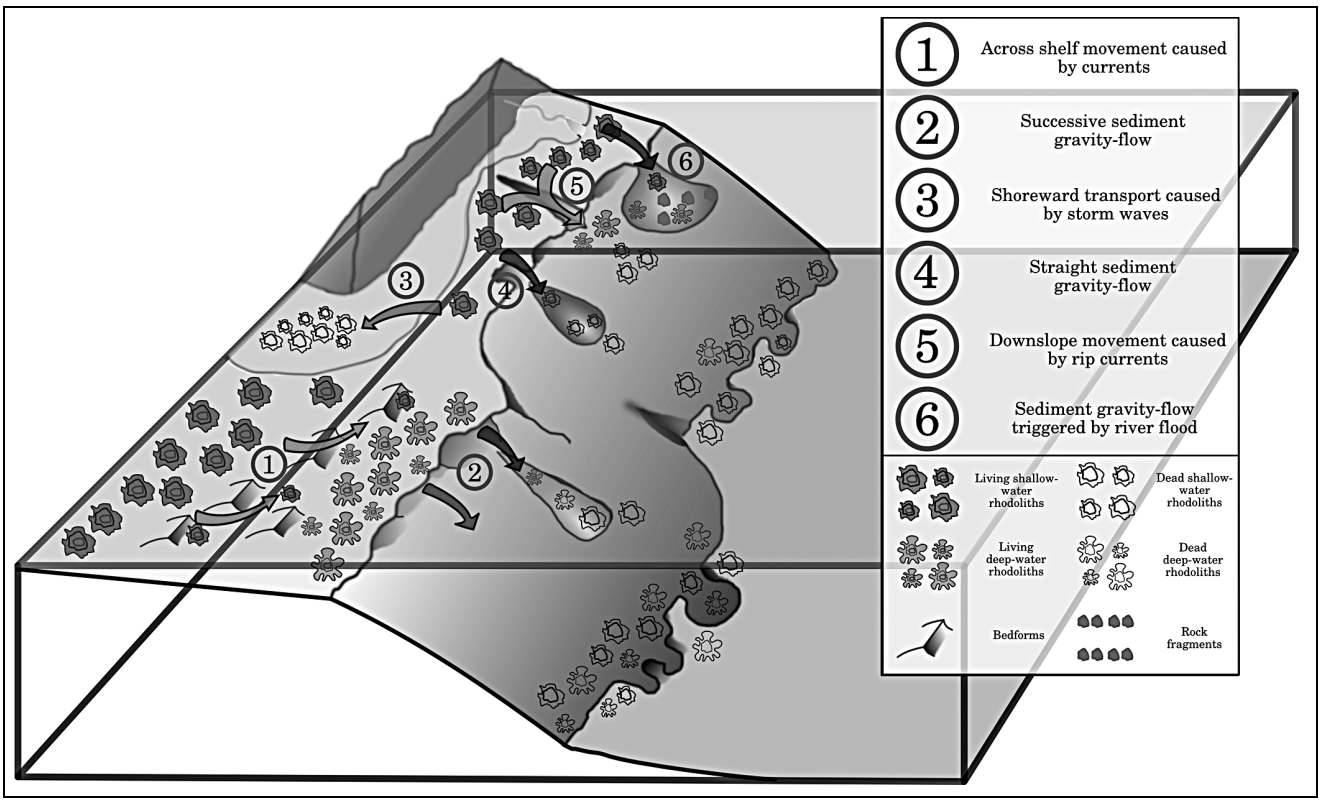

Fig. 12 - Block-diagram summarizing the six main cases of rhodolith transport.

disarticulated, suggesting remobilization of the thanatocenosis before the final burial.

4. Skeletal grain porosities filled by glaucony commonly occur in all of the studied layers of UV, VB, TN and TS outcrops. This mineral forms in marine water below 50-60 m (Odin & Matter 1981; Odin & Fullagar 1988; Carozzi 1993; Amorosi 1997); however, since the fossil association suggests a shallower environment, a transport toward slightly deeper waters is assumed.

5. The presence of deeper-water foraminifers (e.g. *Lenticulina calcar*, Goubert et al. 2001; Murray 2006; Fiorini 2015) and ostracods (Schüttenhelm 1976) mixed with inner platform benthic foraminifers, also suggests a transport toward slightly deeper waters.

Resedimentation is common in rhodalgal platforms and is widely recorded in the fossil record (Pomar et al. 2002; Vigorito et al. 2005; Puga-Bernabéu et al. 2014). Currently, similar processes have also been recorded from the southern tip of Baja California (Mexico), where rhodalgal carbonate is produced in the inner part of the platform and transported into the basin by sediment gravity-flows (Schlanger & Johnson 1969; Halfar et al. 2001). The skeletal composition of the transported material is still similar to the *in situ* assemblage (Van Andel 1964; Schlanger & Johnson 1969). Similar to the PDC limestone, the Baja California carbonate platform also lacks important framework builders (corals are only present in small patches fringing the shoreline) and it is exposed to strong currents. Unlike the Baja California platform, the PDC shallow-water skeletal grains were transported just slightly deeper than their original formation environment. They were moved from inner-middle ramp settings toward at least the lowermost part of the middle ramp, where glaucony formation could take place. Treville gravity-flow deposited in an even deeper environment, probably on the slope.

The transport rate and the carbonate factory exert a significant control over the long-term evolution of the carbonate platform (Pomar & Kendall 2007; Williams et al. 2011). The high transport rate and the presence of a rhodalgal carbonate factory fostered the development of a distally steepened ramp profile in the PDC system. Inherited topographic elements such as elevated areas and depressions must have locally warped this simple profile. According to regional-scale studies, the PDC complex deepens westward and is characterized by NW-SE oriented troughs and highs arranged parallel to the main tectonic lineaments (Schüttenhelm 1976; Dela Pierre et al. 1995). Channels crossing the productive areas of the inner-middle ramp exerted significant control over the facies distribution and the depositional architecture of the system. Sediments were funneled along a VB-Treville northern depression and a Mole-to-Ottiglio southern depression (Schüttenhelm 1976; Fig. 11). Angular clasts from the Casale Monferrato Fm. (Early-Middle Eocene) are common rhodolith

cores, indicating that those rocks were exposed on nearby areas that also influenced the sediment distribution.

Rhodolith Transport

Rhodoliths are precious tools in paleoecological reconstruction of environment with high rate of sediment transport, since they preserve the record of the changing benthic associations through time or space (Basso & Tomaselli 1994; Basso et al. 1998; Checconi & Monaco 2008). Therefore, it is useful to provide a brief overview encompassing the known examples of rhodolith transport from past and present-day oceans.

Transport may be a single or a multiple stage process (Fig. 12). In the latter, rhodoliths and other skeletal grains produced in shallow-water carbonate factories are first moved across the platform under the action of strong currents (Kamp et al. 1988; Puga-Bernabéu et al. 2010; Brandano et al. 2012) (Fig. 12, case 1). Sediment then accumulates on the slope-break and it may eventually move again as sediment gravity-flow (Fig. 12, case 2) (Schlanger & Johnson 1969; Halfar et al. 2001).

During across-platform transport, bioclasts undergo a suite of destructive biostratinomic processes, the most important of which are fragmentation, abrasion, corrosion, size-selection, and biodestruction (Johnson 1962; Staff et al. 1986; Brett & Baird 1986; Wilson 1988; Basso et al. 2009). Rhodoliths may continue to grow by further coralline encrustation or by other constructive biostratinomic processes, which is indicated by sharp contrasts of bioturbation and microfaunal assemblages between the rhodolith nucleus and the rhodolith surface (Basso 1991; Checconi & Monaco 2008; Checconi et al. 2010). Further development of rhodoliths may occur in the time between the deposition near the slope-break and later movements. This period of growth is marked by a sharp change in the algal association of the rhodoliths, with deep water species systematically on the outer layer of the rhodoliths and shallow-water species near the core.

During the subsequent process of sediment gravity-flow, skeletal assemblages may undergo further selection and additional breakage. If the final resting place is within the photic zone, rhodoliths may slowly grow until they are eventually buried. In this situation, a change in both algal assemblage and algae growth form should be detected, with growth forms (of shallow-water species) at the rhodolith nucleus recording frequent overturning, and growth forms (of deep-water species) in rhodolith outer layers that record a less turbulent setting.

During all the stages of the process, skeletal grains may become trapped inside the rhodoliths by either algae binding or by seeping through borings. Although seeping may happen any time, binding only occurs during coralline life. The distribution of skeletal grains inside the rhodoliths is therefore useful to understand whether or not they have formed in the same environment of the algae (Basso 1991).

Single-stage transport is also possible, especially on narrow shelves. Strong storm-induced currents may sweep shallow-water rhodoliths and move them directly into deeper-waters (Fig. 12, case 5) (Checconi et al. 2010; Brandano & Ronca 2014). Also a straight gravity-driven process may carry the rhodoliths directly into the basin (Fig. 12, case 4) (Fravega & Vannucci 1982). The flow may be triggered by seismic activity, strong currents but also by exceptional river floods (Brandano & Ronca 2014) (Fig. 12, case 6). As in the two-stage transport, both destructive biostratinomic processes and new encrustation are always possible until the final burial.

The transport of lithified or partially lithified sediment may also occur. Rhodoliths can be exposed to erosion as a result of uplift or sea-level fall, and the detached elements might move basinward (Leszczyński et al. 2012) similar to other rock fragments (Fig. 12, case 6). The rhodolith-bearing intraclast-rich limestone is likely related to the erosion of lithified or partially lithified sediment.

Channel networks may funnel sediments downslope, leading to the development of channel and channel-related depositional bodies (Cherchi et al. 2000; Vigorito et al. 2005; Vigorito et al. 2006; Bassi et al. 2006).

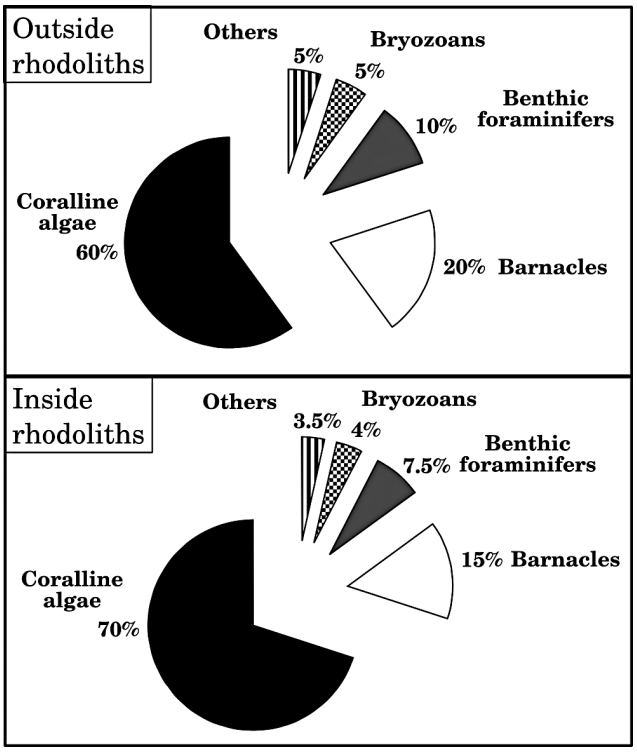

Fig. 13 - Circle charts showing a comparison between the bioclastic composition of the sediment inside and outside rhodoliths; Facies 1.

Shoreward transport, in which shallow-water rhodoliths are moved to the shore by hurricane-generated waves (Johnson et al. 2011), cannot be ruled out (Fig. 12, case 3) since it is known in present-day environments and in the fossil record.

As a general rule, long transport in space and time increases the chance of mixing different materials; longer times also enhance the effects of biostratinomic processes. Transport by gravity flow is likely to be less selective than transport by currents and may allow both rhodoliths and associated skeletal grains to reach deeper settings as a recognizable unit.

In this framework, it is possible to sketch the processes that moved the PDC rhodoliths. The skeletal assemblage observed inside rhodoliths is characterized by shallow-water elements: barnacle fragments, large benthic foraminifers (lepidocyclinids, *Amphistegina*) and small, shallow-water, benthic foraminifers (*E. crispum*, *L. lobatula*). In Facies 1 this assemblage is present both inside the borings at the rhodolith cores (which is generally the oldest part of the coated grain) and within the coralline thalli. The similarity between the skeletal assemblages inside and outside the rhodoliths, in VB, UV, TN and TS outcrops (Fig. 13), indicates negligible mixing effects, which is consistent with a transport mainly caused by sediment gravity-flow. Negligible mixing also point-out to a short distance transport from the formation environment to the final resting place. In Facies 2 the shallow water assemblage is present within coralline thalli and in some bore holes, but glaucony and planktonic foraminifers are present in the borings of the rhodolith outer layers. The lack of planktonic foraminifers and authigenic minerals bound by coralline thalli implies that the final depth of deposition was below the photic zone where rhodoliths could no longer grow. The seeping of deeper water sediment in the bore holes occurred after the death of the rhodoliths.

The absence of a recurring pattern in coralline species assemblages and in growth forms suggests a situation closer to the single-stage transport (Fig 12, case 4), where rhodoliths are moved directly by sediment gravity-flow.

The rhodoliths of Treville, which are interbedded in marls, preserve inside their core the same shallow-water assemblage of skeletal grains of the rhodoliths of UV, VSB, TN and TS (Fig. 5C), testifying that they originated in the same environment. The clear difference between the skeletal assemblage inside the rhodolith and the skeletal assemblage outside the rhodoliths (Fig. 5C, D) is an evidence that the rhodoliths of Treville, unlike those of VB, UV, TN, TS, were transported in a deeper environment, probably on the slope. Obviously coralline-algae growth was impossible in this environment too, and therefore no deep-water material was bound by coralline-algae.

Facies interpretation

Facies 1. The presence of coralline algae and large symbiont-bearing benthic foraminifers (lepidocyclinids, *Amphistegina*, *Operculina*, *Miogypsina*) indicates a formation environment within the photic zone for Facies 1. *E. crispum* is one of the most common benthic foraminifers in all of the lithozones of Facies 1. This species lives between 0 to 50 m (Murray, 2006). The other commonly occurring benthic foraminifers *A. radiata* (20-90 m, Murray 2006); *L. lobatula* (0-150 m, Holcova & Zagorsek 2008), *O. complanata* (50-90 m, Murray 2006) and *Miogypsina* (0-50 m, Geel 2000) indicate a similar depth.

Considering the abundance of barnacle encrustation between coralline layers inside the rhodoliths and on the rhodolith surfaces, environmental conditions were clearly suitable for both coralline algae and barnacles. Large internally compact spherical rhodoliths and the low micrite content suggest the important role of bottom currents in sweeping the ramp on a regular basis. This high-energy environment is also consistent with the barnacle abundance of Facies 1. The growth rate of barnacle has been directly correlated to water turbulence and plankton abundance (Sanford & Menge 2001); barnacle-rich fossil sandstones have been related to turbulent and food-rich environments (Kamp et al. 1988).

The high phosphate content (represented by authigenic phosphate) in lithozone 4 and 5 suggests mesotrophic to eutrophic conditions. The widespread occurrence of authigenic phosphate and glaucony also indicate nutrient-rich waters (Pufahl 2010). Therefore, the studied associations might have developed in non-oligotrophic, high-energy waters. The increase in particulate organic carbon, driven by nutrient abundance, reduces the water transparency and moves the entire benthic zonation shoreward (Hallock & Schlager 1986; Vannucci et al. 2003; Hallock 2005). Melobesioids dominate the PDC coralline algae association (Fig. 2). Currently, similar assemblages are generally found in clear oceanic waters deeper than 60 m (Braga & Aguirre 2001). According to the supposed nutrient abundance and the related water turbidity, we suggest a water-depth of less than 40 m, in the inner-middle ramp, for the formation environment of the rhodoliths of Facies 1. A depth shallower than 40 m is also in accordance with the bathymetric range of the benthic foraminifers association. The final depth of deposition should be placed slightly deeper, in the middle ramp, below 50-60 m, the shallowest depth for the formation of glaucony (Odin & Matter 1981; Odin & Fullagar 1988; Carozzi 1993; Amorosi 1997). Although they were transported, Facies 1 skeletal elements compose a coherent assemblage. Both rhodoliths and most of the smaller bioclastic fragments indicate the same formation environment, as tes-

tified by the presence of the same grain association outside and inside rhodoliths (Fig. 13).

The different skeletal compositions within Facies 1 may be interpreted as variability in sediment supply. The barnacle-dominated rudstone (3UV and 3VB), characterized by the abundance of hard-bottom dweller foraminifers *(Amphistegina* and *Lobatula*), formed in current-exposed areas. The assemblage of the grainstone, rich in lepidocyclinds, epiphytic foraminifers and agglutinated foraminifers (1UV and 1VB), originated in more sheltered zones, possibly with seagrass or other non-calcareous seaweeds.

Facies 2. This facies indicates the inception of sediment starvation after the final drowning of the rhodalgal factory by relative sea-level rise. According to regional studies, this sea-level change initially had a main eustatic component, however, it occurred at the beginning of a long period of tectonic subsidence driven by regional geodynamic processes (Dela Pierre et al. 1995; Bicchi et al. 2006). Therefore, it is difficult to precisely locate this transgression event on the global eustatic curves because of the complex local interplay between tectonic and sea-level fluctuations.

The sea-level rise reduced the sediment supply, by drowning the rhodalgal carbonate factory and by reducing the transport of skeletal material toward the lower parts of the middle ramp. According to the low-stand shedding model (Carannante et al 1996), in carbonate systems dominated by heterozoan production, there is a decrease in sediment transport during high-stand, since the carbonate factory is well below the wave base and therefore wave action is no longer able to move the sediment.

The qualitative analyses suggest that glaucony of this facies has an average degree of maturity. The occurrence of abundant glaucony grains, which are more mature than the light-green grains of Facies 1, is an evidence for the reduced sedimentation rate. Bioturbation processes and long exposure on the seafloor, caused by the low sedimentation rate, allowed fine planktonic sand and glaucony to seep inside the coarse, rhodolith-dominated, underlying deposits.

The rhodoliths of Facies 2 and Facies 1 are similar (shape, size, coralline algae composition, skeletal assemblage inside rhodoliths), suggesting that both rhodolith groups formed in the same environment in the inner-middle ramp and were later transported in the lower middle ramp.

Facies 3. It corresponds to a major sedimentation break in the area. The carbonate production and the sedimentation rate are at their lowest. The massive reduction in carbonate supply is recorded by the transition from the limestone/impure limestone of Facies 1 and Facies 2 to the marly limestone of Facies 3 and 4. Small highly phosphatized rhodoliths swept away from the shallow-water area testify the last transport episodes. Sediment deposited at depth well below 50-60 m, on the lower boundary of the middle-ramp and were exposed for a long time on the sea floor before the final burial, promoting glaucony and phosphate development. Observations of the glaucony grains indicate a high degree of maturity (Fig. 5A). This facies probably represents the maximum flooding surface of the initial marine transgression. According to Amorosi (1995) model, high concentration of mature glaucony in a condensed bed, at the boundary between shallow marine deposits and outer ramp, marks the maximum flooding surface of a marine transgression.

Facies 4. It indicates the onset of hemipelagic sedimentation dominated by calcareous foraminifers, nannofossils and clays. Glaucony occurs in large, deep-green, angular grains and glaucony-filled planktonic foraminifers are common, testifying a still low sedimentation rate. The complete disappearance of coarse, shallow-water skeletal grains suggests a further deepening of the depositional environment.

Conclusions

The studied Burdigalian section (lower unit of Sequence 2, sensu Bicchi et al. 2006) of the PDC represents a carbonate platform developed in a compressional setting where the inner ramp facies are unknown because they were either dismantled and not preserved in place, or buried under younger sediments. The inherited topography exerted a strong control over the facies distribution, depositional profile and pathways of sediment transport. Based on rock texture, mineralogy, chemical composition and fossil content, four main facies were recognized in the studied area. These facies record the evolution of the carbonate factory from maturity to final drowning and dismantling. The relative sea-level rise drowned the ramp and stopped the rhodalgal carbonate factory. This caused a progressive decrease in basinward sediment transport from Facies 1 to 3, with the latter testifying the complete starvation.

The limestone of Facies 1 was composed of large skeletal elements formed in a rhodalgal-dominated inner-middle ramp setting. Currents moved the sediments across the ramp, supplied the energy for rhodolith overturning and produced the water turbulence that the barnacles required to thrive. Sediment gravity-flows carried the sediment basinward in a slightly deeper environment.

The impure limestone of Facies 2 was characterized by an increased contribution of pelagic components and authigenic minerals, indicating the inception of sediment starvation.

The complete sediment starvation was marked by the deposition of the condensed glauconitic-phosphatic limestone of Facies 3. Finally, the sedimentation of the marly limestone of Facies 4, dominated by the planktonic foraminifer tests, prevailed over the entire area.

The study of the skeletal assemblages trapped inside the rhodoliths and of rhodolith characteristics allowed a better reconstruction of the carbonate ramp and its processes. The PDC sediments deposited at a slightly greater depth than their original environment, after a short-lived transport.

Where only rhodoliths are left to witness the presence of a carbonate factory, the material stored inside these nodules may be sufficient to draft the characteristics of that environment. A reconstruction of the platform assemblage and of the major carbonate producers may be achieved based on sedimentary bodies consisting of transported grains as long as it is supported by detailed paleoecological analyses and taphonomy (Nebelsick et al. 2001; Rasser & Nebelsick 2003). The investigation of rhodolith algal assemblages, structure, encrusting organisms and rhodolith-trapped sediment proved to be helpful since rhodoliths are free-living archives that retain all of the information accumulated during their development. Rhodoliths may store a record of their original environment, the platform across which they moved, and their final resting place. When buried and preserved in deeper settings, they may survive the platform and retain a fragment of its history.

Acknowledgments. The authors would like to acknowledge Grazia Vannucci and Sirio Consani for their useful suggestions and support during the long development of this work and the DISTAV of Genova University for their technical support. We would also like to deeply thank Francesco Dela Pierre for his review of an early draft of the manuscript and Anna d'Atri for her detailed revision of the final version of the work. We are grateful to Dario Sartorio and John Buckeridge for their help in the identification of foraminifers and barnacles. Sincere thanks are extended to Agostina Vertino and Valentina Bracchi for their suggestions and support and to Sergio Andò for providing data on the heavy minerals. Special thanks to Chiara Tessarolo and Elisa Malinverno for the fruitful discussions. The authors would also like to thank all of the members of the "Amis d'la Curma" association for their logistical support and friendship. Last, but not least, the authors would also like to extend their special thanks to the editors of the journal for their helpfulness.

REFERENCES

Amorosi A. (1995) - Glaucony and sequence stratigraphy: a conceptual framework of distribution in siliciclastic sequences. *J. Sediment. Res.,* 65(4): 419-425.

Amorosi A. (1997) - Detecting compositional, spatial and temporal attributes of glaucony: a tool for provenance research. *Sediment Geol.,* 109: 135-153.

Adams C.G., Lee D.E. & Rosen R.B. (1990) - Conflicting isotopic and biotic evidences for tropical sea-surface temperatures during the Tertiary. *Palaeogeogr., Palaeoclimatol., Palaeoecol.,* 77: 289-313.

Bassi D., Carannte G., Murru M., Simone L. & Toscano F. (2006) - Rhodalgal/Bryomol assemblage in temperate type carbonate depositional systems: Early Miocene of the Sarcidano area (Sardinia Italy). In: Pedley H. & Carannante G. (Eds) - Cool-Water Carbonate: depositional systems and paleoenvironmental controls. *Geol. Soc. London Spec. Publ.*, 255: 35-52.

Bassi D., Carannante G., Checconi A., Simone L. & Vigorito M. (2010) - Sedimentological and paleoecological integrated analysis of Miocene channelized carbonate margin, Matese Mountains, Southern Apennines, Italy. *Sediment. Geol.*, 230: 105-122.

Basso D. (1991) - Applicazione di un nuovo metodo sperimentale per l'indagine tafonomica in rodoliti attuali: il contributo micropaleontologico. PhD Seminar, V cycle, University of Milan, Milan, 48 pp.

Basso D. (1998) - Deep rhodolith distribution in the Pontinian Islands, Italy, a model for the paleoecology of a temperate sea. *Palaeogeogr., Palaeoclimatol., Palaeoecol.,* 137: 173-187.

Basso D., Fravega P., Piazza M. & Vannucci G. (1998) - Biostratigraphic, paleobiogeographic and paleoecological implications in the taxonomic review of Corallinaceae. *Rend. Lincei*, 9: 201-211.

Basso D., Quaranta F., Vannucci G. & Piazza M. (2012) - Quantification of the coralline carbonate from a Serravallian rhodolith bed of the Tertiary Piedmont Basin (Stazzano, Alessandria, NW Italy). *Geodiversitas*, 34: 137-149.

Basso D. & Tomaselli V. (1994) - Paleoecological potentiality of rhodoliths: a Mediterranean case history. *Boll. Soc. Paleontol. It., Atti del V Simposio di Ecologia e Paleoecologia delle Comunità Bentoniche*, Roma 28-30/9/1992: 17-27.

Basso D., Nalin R. & Nelson C.S. (2009) - Shallow-water *Sporolithon* rhodoliths from North Island (New Zealand). *Palaios*, 24(2): 92-103.

Beavington-Penney S.J., Wright V.P. & Racey A. (2005) - Sediment production and dispersal on the foraminifera-dominated Tertiary ramps: the Eocene El Garia Formation, Tunisia. *Sedimentology*, 52: 537-569.

Bicchi E., Dela Pierre F. & Ferrero E. (2002) - Rosignano e Colma: la Pietra da Cantoni. In: D'Atri A., Dela

Pierre F., Festa A.R., Gnaccolini M., Piana F., Clari P. & Polino R. (Eds) - Tettonica e sedimentazione nel "retroforeland alpino". *Soc. Geol. It.*: 83-89.

Bicchi E., Dela Pierre F., Ferrero E., Maia F., Negri A., Pirini-Radrizzani C., Radrizzani S. & Valleri G. (2006) - Evolution of the Miocene carbonate shelf of Monferrato (North-western Italy). *Boll. Soc. Paleontol. It.*, 45(2): 1-24.

Billups K. & Scheiderich K. (2010) - A synthesis of Oligocene trough Miocene deep sea temperatures as inferred by Mg/Ca ratios. In: Mutti M., Piller W.E. & Betzler C. (Eds) - Carbonate system during the Oligocene-Miocene Climatic Transition. *International Association of Sedimentologist, Spec. Publ.*, 42: 1-16.

Bittner L., Payri C.E., Maneveldt G.W., Couloux A., Cruaud C., Reviers B. & Le Gall L. (2011) - Evolutionary History of the Corallinales (Corallinophycidae, Rhodophyta), inferred from nuclear, plastidial and mitochondrial genomes. *Mol. Phylogenet. Evol.,* 61: 697-713.

Blow W.H. (1969) - Late middle Eocene to Recent planktonic foraminifera biostratigraphy. *Proc. first International conference on planktonic microfossils, Geneve,* 1: 199-422.

Bonci C., Clari P.A., Ferrero E., Ghiribaudo G., Pirini C., Ricci B., Valleri G., & Violanti D. (1990) - The Diatomites of Marmorito (Western Monferrato, Northen Italy). *Mem. Sci. Geol. Univ. Padova*, 42: 189-225.

Borromeo O., Miraglia S., Sartorio D., Bolla E.M., Ortenzi A., Reali S., Castellanos C. & Villalobos R. (2011) - The Perla World-class Giant Gas Field, Gulf of Venezuela; Depositional and diagenetic controls on reservoir quality in Early Miocene carbonates. AAPG International Conference and Exibition, Milan, Italy.

Bosellini A. & Ginsburg R.N. (1971) - Form and internal structure of recent algal nodules (rhodolites) from Bermuda. *J. Geol.,* 79: 669-682.

Bosence D.W.J. (1983a) - Description and classification of rhodoliths (rodoids, rhodolites). In: Peryt T.M. (Ed.) - Coated Grains. Springer-Verlag: 217-224, New York.

Bosence D.W.J. (1983b) - The occurrence and ecology of recent rhodoliths. In: Peryt T.M. (Ed.) - Coated Grains. Springer-Verlag: 225-242, New York.

Bosence D. (2005) - A genetic classification of carbonate platform based on their basinal and tectonic settings in the Cenozoic. *Sediment. Geol.*, 175: 49-72.

Braga J.C. & Aguirre J (2001) - Coralline algal assemblages in Upper Neogene reef and temperate carbonates in Southern Spain. *Palaeogeogr., Palaeoclimatol., Palaeoecol.,* 175(1): 37-41.

Braga J.C., Bassi D. & Piller W. E. (2010) - Paleoenvironmental significance of Oligocene-Miocene coralline red algae - a review. In: Mutti M., Piller W.E. & Betzler C. (Eds) - Carbonate system during the Oligocene-Miocene Climatic Transition. *International Association of Sedimentologist, Spec. Publ.*, 42: 165-182.

Brandano M., Vannucci G., Pomar L. & Obrador A. (2005) - Rhodolith assemblages from the lower Tortonian carbonate ramp of Menorca (Spain): environmental and paleoclimatic implications. *Palaeogeogr., Palaeoclimatol., Palaeoecol*, 226: 307-323.

Brandano M., Vannucci G. & Mateu-Vicens G. (2007) - Le Alghe rosse calcaree come indicatori paleoambientali: l'esempio della rampa carbonatica Laziale-Abruzzese (Burdigaliano, Appennino centrale). *Boll. Soc. Geol. It.,* 126(1): 55-69.

Brandano M., Frezza V., Tommasetti L., Pedley. M. & Matteucci R. (2009) - Facies analysis and paleoenvironmental interpretation of the Late Oligocene Attard Member (Lower Coralline Limestone Formation), Malta. *Sedimentology*, 56: 1138-1158.

Brandano M., Lipparini L., Campagnoni V. & Tomassetti L. (2012) - Downslope-migrating larges dunes in the Chattian carbonate ramp of the Majella Mountains (Central Apennines, Italy). *Sediment. Geol.*, 255-256: 29-41.

Brandano M. & Ronca S. (2014) - Depositional processes of the mixed carbonate-siliciclastic rhodolith beds of the Miocene Saint-Florent Basin, northern Corsica. *Facies*, 60: 73-90.

Brett C.E. & Baird G.C. (1986) - Comparative taphonomy: a key to paleoenvironmental interpretations based on fossils preservation. *Palaios* 1: 207-227.

Carannante G., Esteban M., Milliman J.D. & Simone L. (1988) - Carbonate lithofacies as paleolatitude indicators: problems and limitations. *Sediment. Geol.*, 60: 333-346.

Carannante G., Severini C. & Simone L. (1996) - Off shelf carbonate transport along foramol (temperate-type) open shelf margin: an example from the Miocene of the central and southern Apennines (Italy). *Mem. Soc. Geol. Fr.,* 169: 277-288.

Carannante G., Graziano R., Pappone G., Ruberti D. & Simone L. (1999) - Depositional System and Response to Sea Level Oscillation of the Senonian Rudist-bearing Carbonate shelves. Examples from Central Mediterranean Area. *Facies*, 40: 1-24.

Carozzi A.V. (1993) - Sedimentary Petrography. Prentice Hall, Englewood Cliffs, NJ, 263 pp.

Civitelli G. & Brandano M. (2005) - Atlante delle litofacies e modello deposizionale dei calcari a Briozoi e Litotamni della piattaforma carbonatica Laziale-Abruzzese. *Boll. Soc. Geol. It.*, 124: 611-643.

Checconi A. & Monaco P. (2008) - Trace fossil assemblages in rhodoliths from the Middle Miocene of Mt. Camposauro (Longano Formation, Southern Appenines, Italy). *Studi Trentini Sci. Nat. Acta Geol.*, 83: 165-176.

Checconi A., Bassi D., Carannante G. & Monaco P. (2010) - Re-deposited rhodoliths in the Middle Miocene hemipelagic deposits of Vitulano (Southern Appenines, Italy): Coralline assemblage characterization and related trace fossils. *Sediment. Geol.*, 225: 50-66.

Cherchi A., Murru M. & Simone L. (2000) - Miocene Carbonate Factories in the Sy-rift Sardinia Graben Subbasin (Italy). *Facies*, 43: 223-240.

Clari P., Dela Pierre F., Novaretti A. & Timpanelli M. (1994) - La successione oligo-miocenica del Monferrato occidentale: confronti e relazioni con il Monferrato o-

rientale e la Collina di Torino. *Atti Ticinesi Sci. Terra Serie Spec.*,1: 192-203.

Clari P., Dela Pierre F., Novaretti A. & Timpanelli M. (1995) - Late Oligocene-Miocene sedimentary evolution of the critical Alps-Apennines junction: the Monferrato area, Northwestern Italy. *Terra Nova*, 7: 144-152.

Clarke K.R. & Gorley R.N (2006) - PRIMER v6: User Manual/Tutorial. PRIMER-E, Plymouth, 192 pp.

Coletti G., Basso D. & Frixa A. (in press) - Economic importance of coralline carbonates. In: Riosmena-Rodriguez R., Nelson W. & Aguirre J. (Eds) - Rhodolith/Maerl beds: a global perspective. Special volume, Springer-Verlag, Berlin.

D'Atri A. (1990) - Facies e sequenze deposizionali nella Formazione di Visone (Miocene inferiore, Bacino Terziario Ligure Piemontese). *Mem. Soc. Geol. It.*, 45: 723-729.

D'Atri A., Dela Pierre F., Lanza R. & Ruffini R. (1999) - Distinguishing primary and resedimented vitric volcanoclastic layers in the Burdigalian carbonate shelf deposits in Monferrato (NW Italy). *Sediment. Geol.*, 129: 143-163.

D'Atri A., Dela Pierre F., Novaretti A., Cosca M.A. & Hunziker J.C. (2001) - Miocene plankton biostratigraphy and $^{40}Ar/^{39}Ar$ dating. *Eclogae Geol. Helv.,* 94(2): 137-144.

Dela Pierre F., Mikhailov V. & Polino R. (1995) - The tectonosedimentary evolution of the tertiary basin in the western Po plain: Kinematics inferred from subsidence curves. *Atti del Convegno "Rapporti tra Alpi e Appennino" Peveragno (CN), Acc. Naz. Sci., Collana Scritti e Documenti*, XIV: 129-146.

Dela Pierre F., Piana F., Fioraso G., Boano P., Bicchi E., Forno M.G., Violanti D., Balestro G., Clari P., D'Atri A., De Luca D., Morelli M. & Ruffini R. (2003) - Note illustrative della carta geologica d'Italia alla scala 1:50000; Foglio 157 Torino. Apat e Dipartimento per la Difesa del Suolo, 147 pp.

Erlich R.N., Barrett S.F. & Ju G.B (1990) - Seismic and geologic characteristics of drowning events on carbonate platforms. *AAPG Bull.*, 74: 1523-1537.

Falletti P., Gelati R. & Rogledi S. (1995) - Oligo-Miocene evolution of Monferrato and Langhe related to deep structures. *Atti del Convegno "Rapporti tra Alpi e Appennino" Peveragno (CN), Accademia Nazionale delle Scienze, Collana Scritti e Documenti,* XIV: 1-19.

Field J.G., Clarke K.R. & Warwick R.M. (1982) - A pratical strategy for analyzing multispecies distribution patterns: *Mar. Ecol. Progr. Ser.*, 8: 37-52.

Fiorini F. (2015) - Recent benthic foraminifera from the Caribbean continental slope and shelf off west Colombia. *J. South Amer. Earth Sci.*, 60: 117-128.

Flügel E. (2009) - Microfacies of Carbonate Rocks: Analysis Interpretation and Application. Springer Verlag, 1007 pp.

Fournier F. & Borgomano J. (2007) - Geological significance of seismic reflections and imaging of the reservoir architecture in the Malampaya gas field (Philippines). *AAPG Bull.*, 91: 235-258.

Fravega P. & Vannucci G. (1982) - Significato e caratteristiche degli episodi a rhodoliti al top del Serravalliano tipo. *Geol. Romana*, 21: 705-715.

Geel T (2000) - Recognition of stratigraphic sequences in carbonate platform and slope deposits: empirical models based on microfacies analysis of Paleogene deposits in southeastern Spain. *Palaeogeogr., Palaeoclimatol., Palaeoecol.,* 155: 211-238.

Goubert E., Nèraudeu D., Rouchy J.M. & Lacour D. (2001) - Foraminiferal record of environmental changes: Messinian of the Los Yeos area (Sorbas Basin, SE Spain). *Palaeogeogr., Palaeoclimatol., Palaeoecol.*, 175: 61-78.

Halfar J., Godinez-Orta L., Goodfriend G.A., Mucciarone D.A., Ingle J.C. Jr. & Holen P. (2001) - Holocene-late Pleistocene non-tropical carbonate sediments and tectonic history of the western rift basin margin of the southern Gulf of California. *Sediment. Geol.*, 144: 149-178.

Halfar J. & Mutti M. (2005) - Global dominance of coralline red-algal facies: A response to Miocene oceanographic events. *Geology*, 33: 481-484.

Hallock P. & Schlager W. (1986) - Nutrient excess and the demise of coral reefs and carbonate platforms. *Palaios*, 1: 389-398.

Hallock P. (2005) - Global change and modern reefs: new opportunities to understand shallow-water carbonate depositional processes. *Sediment. Geol.*, 175: 19-33.

Heubeck C., Story K., Peng P., Sullivan C. & Duff S. (2004) - An integrated reservoir study of the Liuhua 11-1 field using a high-resolution three-dimensional seismic data set. In - Seismic imaging of carbonate reservoirs and systems. *AAPG Mem.*, 81: 149-168.

Holcová K. & Zágoršek K (2008) - Bryozoa, foraminifera and calcareous nannoplankton as environmental proxies of the "bryozoan event" in the Middle Miocene of Central Paratethys (Czech Republic). *Palaeogeogr., Palaeoclimatol, Palaeoecol.*, 267: 216-234.

Johnson R.G (1962) - Mode of Formation of marine fossil assemblage of the Pleistocene Millerton Formation of California. *Geol. Soc. Am. Bull*, 73: 113-130.

Johnson M.E., Da Silva C.M., Santos A., Baaril B.G., Cachão M., Mayoral E.J., Rebelo A.C. & Ledesma-Vàsquez J. (2011) - Rhodoliths transport and immobilization on a volcanically active rocky shore: Middle Miocene at Cabeço das Laranjas on Ilhéu de Cima (Madeira Archipelago, Portugal). *Palaeogeogr., Paleoclimatol., Paleoecol.,* 300: 113-127.

Kamp P.J.J., Harmsen F.J., Nelson C.S. & Boyle S.F. (1988) - Barnacle-dominated limestone with giant cross-beds in a non tropical, tide swept, Pliocene forearc seaway, Hawke's Bay, New Zealand. *Sediment. Geol.*, 60: 173-195.

Kato A., Baba M. & Suda S. (2011) - Revision of the Mastophoroideae (Corallinales, Rhodophyta) and Polyphyly in the nongeniculate species widely distributed on pacific coral reefs. *J. Phycol.*, 47: 662-672.

Kruskal J.B. (1977) - Multidimensional scaling and other methods for discovering structure. In: Enslein K.,

Ralston A. & Wilf H.S. (Eds) - Statistical methods for digital computers: 296-339. Wiley, New York.

Lee D.E., Scholz J. & Gordon D.P. (1997) - Paleoecology of a late Eocene mobile rockground biota from North Otago, New Zealand. *Palaios*, 12: 568-581.

Leszczyński S., Kołodziej B., Bassi D., Malata E. & Gasiński M.A. (2012) - Origin and resedimentation of rhodoliths in the Late Paleocene of the Polish Outer Carpathians. *Facies*, 58: 367-387.

Loeblich A.R. & Tappan H. (1987) - Foraminiferal Genera and Their Classification. Van Nostrand Reinhold, New York, 1820 pp.

Maffione M., Speranza F., Faccenna C., Cascella A., Vignaroli G. & Sagnotti L. (2008) - A syncronous Alpine and Corsica-Sardinia rotation. *J. Geophys. Res*., 113. doi: 10.1029/2007JB005214.

Major J.J. (1998) - Pebble orientation on large, experimental debris-flow deposits. *Sediment. Geol.,* 117: 151-164.

Mosca P., Polino R., Rogledi S. & Rossi M. (2009) - New data from the kinematic interpretation of Alps-Appenines junction (Northwestern Italy). *Int. J. Earth Sci.*, 99: 833-849.

Mosbrugger M., Uterscher T. & Dilcher D.L. (2005) - Cenozoic continental climatic evolution of Central Europe. *Proc. Nat. Acad. Sci. U.S.A*., 102(42): 14964-14969.

Murray J. (2006) Ecology and Applications of Benthic Foraminifera. Cambridge University Press, 426 pp.

Mutti E., Bernoulli D., Ricci Lucchi F. & Tinterri R. (2009) - Turbidite and turbidity currents: from Alpine flysch to the exploration of continental margins. *Sedimentology,* 56: 267-318.

Nebelsick J.H., Stingl V. & Rasser M. (2001) - Autochthonous facies and allochthonous debris flows compared: Early Oligocene Carbonate facies patterns of the lower Inn Valley (Tyrol, Austria). *Facies*, 44: 31-46.

Neuhaus D., Borgomano J., Jauffred J.C., Mercadier C., Olotu S. & Grotsch J. (2004) - Quantitative Seismic Reservoir Characterization of an Oligocene-Miocene Carbonate Buildup: Malampaya Field, Philippines. In: Eberli G.B., Masaferro J.L. & Sarg J.F. (Eds) - Seismic imaging of carbonate reservoirs and systems. *AAPG Mem*., 81: 169-183.

Newman A.W. & Ross A. (1976) - Revision of the balanomorph barnacles including a catalog of the species. *Mem. San Diego Soc. Nat. Hist.,* 9: 1-108.

Novaretti A., Bicchi E., Condello A., Ferrero E., Maia F., Tonon M. & Torta D. (1995) - La successione oligomiocenica del Monferrato: sintesi dei dati biostratigrafici. Atti del Convegno "Rapporti tra Alpi e Appennino" Peveragno (CN). *Acc. Naz. Sci., Collana Scritti e Documenti*, XIV: 39-59.

Odin G.S. & Matter A. (1981) - De glauconiarum origine. *Sedimentology*, 28: 611-641.

Odin G.S. & Fullagar P.D. (1988) - Geological significance of the glaucony facies. In: Odin G.S. (Ed.) - Green Marine Clay: 295-332. Elsevier, Amsterdam.

O'Herne L. (1974) - A reconsideration of *Amphistegina lessonii* d'Orbigny, 1826, sensu Brady, 1884 (Foraminifera). *Scripta Geol*., 26: 1-53.

Parson-Hubbard K.M., Callender W.R., Powell E.N., Brett C.E., Walker S.E., Raymond A.L. & Staff G.M. (1999) - Rates of burial and disturbance of experimentally deployed mollusks: Implications for preservation potential. *Palaios*, 14: 337-351.

Paull C.K., Ussler W., Greene H.G., Keaten R., Mitts P. & Barry J. (2003) - Caught in the act: the 20 December 2001 gravity flow event in the Monterey Canyon. *Geo-Marine Letters*, 22: 227-232.

Pomar L., Obrador A. & Hildegard W. (2002) - Sub-wavebase cross bedded grainstone on adistally steepeend carbonate ramp, Upper Miocene, Menorca, Spain. *Sedimentology*, 49: 139-169.

Pomar L. & Kendall C.G.St.C. (2007) - Architecture of carbonate platforms: a response to hydrodynamics and evolving ecology. Control on carbonate platform and reef development. *SEPM Spec. Publ*., 89: 187-216.

Pufahl P.K. (2010) - Bioelemental sediments In: James N.P. & Darlymple R.W. (Eds) - Facies Models 4. *Geol. Assoc. Canada Spec. Publ.*, 6: 477-503.

Puga-Bernabéu A., Martín J.M., Braga J.C. & Sánchez-Almazo I.M (2010) - Downslope-migrating sandwaves and platform-margin clinoforms in a current-dominated, distally steepened temperate-carbonate ramp (Guadix Basin, Southern Spain). *Sedimentology*, 57: 293-311.

Puga-Bernabéu A., Martín J.M., Braga J.C. & Aguirre G. (2014) - Offshore remobilization processes and deposits in low-energy temperate-water carbonate-ramp systems: examples from the Neogene bains of the Betic Cordillera (SE Spain). *Sediment. Geol*., 304: 11-27.

Rasser M.W. & Nebelsick J.H. (2003) - Provenance analysis of Oligocene autochthonous and allochthonous coralline algae: a quantitative approach towards reconstructing transported assemblages. *Palaeogeog., Palaeoclimatol., Palaeoecol*., 201: 89-111.

Rossi M., Mosca P., Polino R., Rogledi S. & Biffi U. (2009) - New outcrop and subsurface data in the Tertiary Piedmont Basin: unconformity-bounded stratigraphic units and their relationships with basin-modification phases. *Riv. Ital. Paleontol. Strat*., 115: 305-335.

Ruffini R. (1995) - Evidenze di attività vulcanica terziaria nelle Alpi occidentali: problemi ed ipotesi. PhD thesis. Università di Torino, Turin, Italy, 160 pp.

Sanford E. & Menge B.A. (2001) - Spatial and temporal variation in barnacle growth in coastal upwelling system. *Mar. Ecol. Progr. Ser*., 209: 143-157.

Sattler U., Zampetti V., Schlager W. & Immenhauser A. (2004) - Late leaching under deep burial conditions: a case study from the Miocene Zhujiang Carbonate Reservoir, South China Sea. *Mar. Petrol. Geol.*, 21: 977-992.

Schlager W. (2003) - Benthic carbonate factories of the Phanerozoic. *Int. J. Earth Sci*., 92: 445-464.

Schlanger S.O. & Johnson C.J. (1969) - Algal banks near La Paz, Baja California - Modern Analogues of source areas of transported shallow water fossils in Pre-Alpine flysch depostis. *Palaeogeogr., Palaeoclimatol., Palaeoecol*., 6: 141-157.

Schüttenhelm R.T.E. (1976) - History and modes of Miocene carbonate deposition in the interior of the Piedmont Basin, NW Italy. PhD thesis. *Utrecth Micropaleontol. Bull.*, 4, 207 pp., Utrecth.

Sneed E.D. & Folk R.L. (1958) - Pebbles in the Colorado River, Texas, a study of particle morphogenesis. *J. Geol.*, 66(2): 114-150.

Staff G.M., Stanton R.J. Jr., Powell E.N. & Cummins H. (1986) - Time-averaging, taphonomy and their impact on paleocommunity reconstruction: death assemblages in Texas bays. *Geol. Soc. Am. Bull.*, 97: 428-443.

Steneck R.S. (1986) - The ecology of Coralline Algal Crusts: Convergent Patterns and Adaptive Strategies. *Ann. Rev. Ecol. Syst.,* 17: 273-303.

Vahrenkamp V.C., David F., Duijndam P., Newall M. & Crevello P. (2004) - Growth architecture, faulting, and karstification of a middle Miocene carbonate platform, Luconia Province, offshore Sarawak, Malaysia. *AAPG Mem.*, 81: 329-350.

Van Andel Tj.H. (1964) - Recent marine sediments of Gulf of California. In: Van Andel Tj.H. (Ed.) - Marine Geology of the Gulf of California. *AAPG Mem.*, 3: 216-310.

Vannucci G., Piazza M., Fravega C. & Abate C. (1996) - Litostratigrafia e paleoecologia di successioni a rodoliti della Pietra da Cantoni (Monferrato Orientale, Italia Nord-Occidentale). *Atti Soc. Toscana Sci. Nat. Mem., Serie A*, 103: 69-86.

Vannucci G., Quaranta F., Piazza M. & Fravega P. (2003) - The Oligocene reefal facies of Bric San Bernardino (Millesimo, NW Italy). Le facies recifali oligoceniche di Bric San Bernardino (Millesimo, Italia nord-occidentale). *Atti Ticinesi Sci. Terra*, 44: 35-44.

Vigorito M., Murru M. & Simone L. (2005) - Anatomy of a submarine channel system and related fan in a foramol/rhodalgal carbonate sedimentary setting: a case history from the Miocene syn-rift Sardinia Basin (Italy). *Sediment. Geol.,* 174: 1-30.

Vigorito M., Murru M. & Simone L. (2006) - Architectural patterns in a multistorey mixed carbonate-siliciclastic submarine channel, Porto Torres Basin, Miocene, Sardinia, Italy. *Sediment. Geol.*, 186: 213-236.

Wade B.S., Pearson P.N., Berggren W.A. & Pälike H. (2011) - Review and revision of Cenozoic tropical planktonic foraminiferal biostratigraphy and calibration to the geomagnetic polarity and astronomical time scale. *Earth-Sci. Rev.*, 104: 111-142.

Williams H.D., Burgress P.M., Wright V.P., Della Porta G. & Granjeon D. (2011) - Investigating carbonate platform types: multiple controls and a continuum geometries. *J. Sed. Res.*, 81: 18-37.

Wilson M.V.H. (1988) - Taphonomic processes: information loss and information gain. *Geosci. Canada*, 15(2): 131-148.

Zingg T. (1935) - Beitrag zur Schotteranalyse. *Schweiz. Miner. Petrog.*, 15: 39-140.